Chapter 7: Formulation development & optimization

7.0 Formulation Development & Optimization

7.1 Introduction

The amelioration of the unmet need in effective treatment of cancer necessitates the delivery of the therapeutic agents to the required sites of action (1). One of the current treatment options include the usage of multiple agents acting on same or different molecular targets to ensure better tumor cell killing outcomes. Importantly, mere parenteral administration of such drug combinations may not be sufficient to elicit the desired response and may be associated with increased toxicity to the human system (2). Further, the difference in the pharmacokinetic (PK)-pharmacodynamic (PD) profiles of the individual drugs results in absence of simultaneous effective presence of the drugs at the disease site. The attainment of specificity in drug delivery presenting altered pharmacokinetic profiles may be achieved by exploring the nanocarrier platforms for improved temporospatial presence (3). While various lipid and polymer based nanoparticulate approaches have been evaluated pre-clinically, the liposomes have been widely used clinically in the safer and effective delivery of antineoplastic agents to the tumor sites (4). These biodegradable biocompatible phospholipid-based nanovesicles may be modulated to present suitable drug encapsulation properties based on the lipophilicity of the drugs (internal aqueous core, lipid bilayer, peri-liposomal space) (5). Presentation of drugs through nanoliposomes increases the systemic drug half-lives while presenting with reduced as well as manageable toxicity profiles leading to reduction in the effective payload being administered to the patients. Importantly these nanoliposomes may be surface engineered against disease targets to have increased active presentation at the loci of action (4). Further, these nanocarriers may be modulated for carrying multiple drugs loaded in particular molar ratios to improve the efficacy of such therapeutic combinations (6). Although, the nanoliposomal delivery of antineoplastic agents have presented encouraging effective results, the lack of appropriate formulation design has resulted in non-attainment of the intended clinical outcomes (eg. Lipoplatin™, Alocrest™, Brakiva™ among others) (7). Consequently, it is important to have optimized nanoformulations of intended therapeutic agents having adequate encapsulation efficiency, particle size, zeta potential, morphology and drug release for effective treatment. A

quality-by-design (QbD) approach may be used for building in the intended quality target product profile (QTPP) by establishing a correlation between the dependent variables and the independent variables [(critical material attributes (CMA) and critical process parameters (CPP)]. These effective nanoformulations may be prepared through use of screening and design of experiments (DOE) based optimization of the CMA and CPP. The physiochemical properties and chemical structure of the therapeutic agents would play an important role in determination of the appropriate nanoliposomal components. Hydrophilic drugs may be passively loaded/equilibrated into aqueous core of the liposomes, amphipathic weak acids/bases and those having protonizable amino groups have presented suitable opportunities for active loading into the same compartment. The choice of remote loading approaches would further entail the presence of appropriate transmembrane salt, metal ion and pH gradient among others (8). The hydrodynamic diameter and surface potential of the liposomes plays an important role in the determination of the drug loading capacities, their biodistribution and drug release profiles while being affected by the choice of the phospholipid and the content of cholesterol (9). Majority of the clinically approved liposomal formulations have being formulated using bilayer forming phosphatidylcholines, phophatidylglycerols, bilayer stabilizing cholesterol and presence/absence of pegylated lipids (7). The drug loading efficiency, stability, release characteristics and biofate of nanoliposomes would further be affected by various properties of the bilayer forming phosphatidylcholines. These include the alkanoyl substitution of the glycerophosphoric acid and its side chain length; presence of saturated/unsaturated fatty acid substitutions; charge of lipid; degree of formation of lamellar crystalline structures as well as packing parameter (P) and temperature of sol-gel transition (T_c) (10). The selection of the phospholipids would further require the assessment of the toxicity and immunogenicity profile upon intravenous administration. The physicochemical properties of the liposomes would further be affected by the presence and level of amphipathic cholesterol which has been implicated for the modulation of bilayer membrane permeability, stability and fluidity by plugging the gaps in imperfect packing pf the phospholipids (11).

The nanoliposomal drug release characteristics may be modulated according to disease targets and would be affected by leakage profile as a function of the carrier membrane stability. The

destabilization of the bilayer membrane integrity is affected by rate of hydrolysis as well as peroxidation of the saturated/unsaturated lipidic components by physiological phospholipases (12). The drug release profiles are affected by the similar factors which affect the drug loading and both these parameters may be optimized to meet the particular requirements of the formulation (13).

The loading and release from the nanoliposomes are further affected by the physicochemical properties of drugs. The loading (active/passive) of therapeutic agents are dependent on the chemical structure (presence of ionizable nitrogen atoms), dissociation constants (pK), logarithmic value of partition coefficient (log P) and degree of ionization at drug loading pH among others (8). Consequently, the optimization approaches of nanoliposomal formulations would entail rationale-based evaluation of various CPP and CMA for imparting the desired physicochemical properties to the drug carrier. Additionally, careful assessment of factors needs to be done for ascertaining the intended plasma circulation time, in-transit biological stability, optimal release kinetics and bioavailability of therapeutic agent at the tumor site, Importantly, while issues related to active loading of single drug in a nanocarrier has been widely described in literature, the simultaneous remote loading of two drugs exhibits various challenges associated with both drugs individually and present together (14).

The present chapter is intended to explore a systematic QbD approach to co-encapsulate two cell cycle specific drugs Doxorubicin and Vincristine in a single liposome which evaluating the impact of the variation of the independent variables (CPP and CMA) on that of the intended dependent variables. Based on previously published literature, the initial cause effect analysis (Ishikawa diagram) was analysed and the effect of the independent variables on the dependent responses (Encapsulation efficiency of Dox, VCR, particle size and zeta potential) were evaluated using One-factor at a time (OFAT) study (Figure 25). The independent variables evaluated for the active co-loading of the drugs included transmembrane salt gradient, concentration of cholesterol (lipid molar ratio), drug loading temperature, phosphatidylcholine chain length, sequence of addition of drugs, pH of drug loading, external medium, drug to lipid molar ratio and concentration of Ammonium sulphate. In addition to the aforementioned

responses for co-loaded formulations having an encapsulation efficiency of more than 85% of both drugs, morphological evaluation using cryo-Transmission Electron Microscopy (cryo-TEM) and drug release was evaluated at various pH (7.4, 5.5). Further, this research approach is intended to present the development of combinatorial nanoliposomes having ease of scalability to cGMP scales.

7.2 Material and Methods

7.2.1 Materials

Hydrogenated soy phosphatidylcholine (HSPC), 1,2-distearoyl-sn-glycero-3-phosphocholine (DSPC) and pegylated lipid1,2-distearoyl-sn-glycero-3-phosphoethanolamine-N[methoxy(polyethyleneglycol)2000] (mPEG-DSPE) were procured from Lipoid GmbH (Ludwigshafen, Germany). 1,2-dimyristoyl-sn-glycero-3-phosphocholine (DMPC) and 1,2-dipalmitoyl-sn-glycero-3-phosphocholine (DPPC) were obtained as gift samples form Avanti Polar Lipids (Alabama, USA) 1,2-Arachinoyl-sn-glycero-3-phosphocholine (DAPC) was purchased from Corden Pharma (Liestal, Switzerland). Cholesterol was obtained from Dishman BV (Netherlands). Ammonium sulphate, ammonium phosphate, ammonium citrate, copper sulphate, Ethylenediaminetetraacetic acid diammonium salt, histidine, sucrose and Triethanolamine was purchased from Merck KGaA (Darmstadt, Germany). Sulphobutylether Beta-Cyclodextrin ammonium salt and copper gluconate was purchased from Biophore India Pharmaceuticals (Hyderabad, India) and Spectrum Chemicals Mfg Corp (New Jersey, USA) respectively. Vincristine sulphate (VCR) was purchased from Minakem (Beuvry-la-Forêt, France) while Doxorubicin Hydrochloride (DOX) was obtained from Synbias Pharma AG (Mannheim, Germany). Dehydrated alcohol was purchased from Commercial Alcohols (Ontario, Canada). All other chemicals used in the study were of analytical grade.

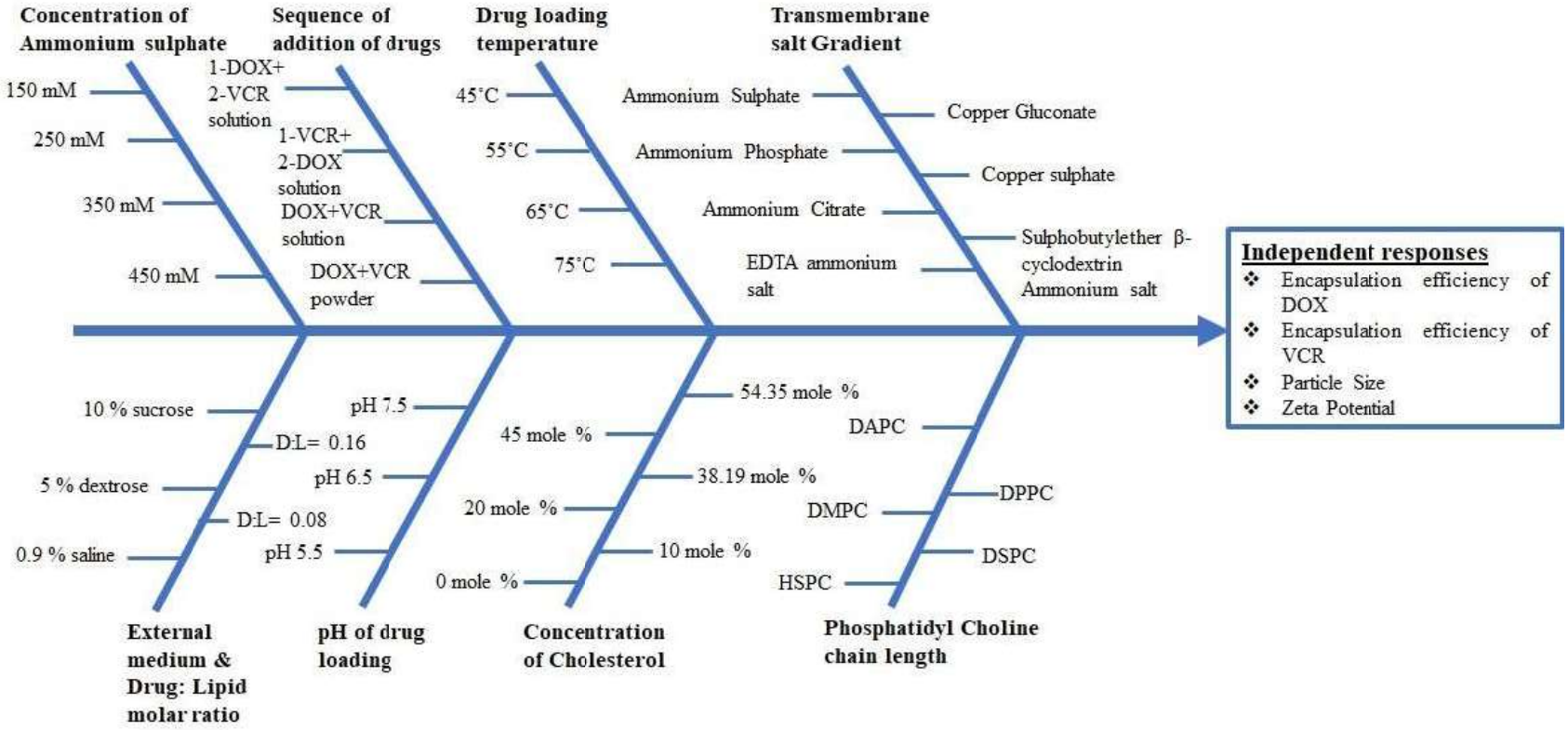

Figure 25: Ishikawa diagram linking the effect of independent variables on co-loading of two drugs to dependent responses.

7.2.2 Liposome preparation and active drug loading

The liposomes were prepared by the traditional ethanolic injection method and the important independent factors which may affect the formulation characteristics were intially screened by OFAT (one-factor-at-a time) studies (Table 16). The common method for the preparation for the blank liposomes have been prepared as detailed earlier (15). Briefly, the phosphocholine lipid component, cholesterol and mPEG 2000-DSPE in molar ratios as mentioned in the OFAT studies was weighed accurately in a clean glass vial, added with 8% v/v of dehydrated alcohol and heated to 65±5°C for ensuring the solubilization of the lipids. The aqueous solution of hydration salts (as mentioned in OFAT studies) was prepared by dissolving the required quantity of the salt in water for injection at 25±3°C. The temperature of the hydration buffer solution was increased to 65±5°C and stirred at 400-500 rpm (IKA, Staufen, Germany). The blank multilamellar vesicles (MLV) were prepared by taking the ethanolic lipid solution in a syringe and injecting rapidly into the hydration buffer solution under stiring at 400-500 rpm at 65±5°C. The formed liposomal suspension were incubated under 300-400 rpm at 65±5°C for 30 minutes. The size of MLVs was reduced using thermobarrel pneumatic extruder (Evonik, Ontario, Canada) maintained at a temperature of ten degrees higher than the phase transition temperature of the phosphocholine component in the liposomal formulation (DMPC at 35±5°C; DPPC at 55±5°C; HSPC, DSPC at 65±5°C; DAPC at 75±5°C). The size reduction to unilamellar vesicles (ULV) to 100±20 nm was effected using two passes through 4 stacks of 0.2 µ and finally 6 passes through 4 stacks of 0.08 µ polycarbonate membrane (Cytiva, Uppsala, Sweden). The liposomal suspension was cooled to 25±3°C and external unentrapped salt was exchanged with intended external medium (10% sucrose/ 5% Dextrose/ 0.9% Saline) using ultrafiltration (Cytiva, Uppsala, Sweden).The removal of the external salt aids in the creation of the transmembrane gradient necessary for the active loading of the drugs. The cholesterol content of the liposomes were determined using RP-HPLC (Agilent, California, USA)) and drugs (DOX, VCR) were weighed in glass vials active loading at drug-lipid molar ratios of 0.14 (DOX:lipid) and 0.04 (VCR:lipid) (16). The drugs were dissolved in external medium solution at temperatures above the phase transition temperature (as mentioned during size reduction process). The calculated quantity of blank liposomal suspension was taken in

glass vial, pH was adjusted to intended values (5.5, 6.5, 7.5) using histidine and incubated with the drug solutions (except for batch no. T22, where drugs were added as powder) at 65±5°C for 1 hour under stirring at 300-400 rpm (IKA, Germany). Post active loading, the liposomal suspension was rapidly cooled to 2-8°C using an ice bath and then further held at this temperature for 1 hour. The temperature of the suspension was then raised to 25±3°C and the volume was made up to the determined batch size with external medium solution. The liposomal suspension was aseptically filtered through 0.2µ PES membrane filter (Pall Corporation, New York, USA).

7.2.3 Entrapment efficiency

The quantification of the drugs in the liposome was evaluated simultaneously using reverse phase high performance liquid chromatography (HPLC, Agilent, California, USA) as per previously described methods (15, 17). Briefly, methanol was used to disrupt the liposomal bilayer to get the entire drug content (DOX, VCR) in solution. Then gradient elution technique through C18 column was used to detect both the drugs (assay of drugs) at 254 nm UV detector (Retention time of drugs- DOX:4-6 minutes; VCR: 7-9 minutes). Reverse phase column (150 X 4.6 mm, 3.5µ symmetry shield, Waters, USA) was used while the flow rate of the mobile phase was maintained at 1.0 ml/min using Agilent 1100 series (Agilent, California, USA). Gel filtration chromatography columns Superdex 75 (GE healthcare, Singapore) was used for the separation of the free drug from the liposomal entrapped components and the content was evaluated for the entrapped drug content. The liposomal suspension (0.5 ml) was added to the columns and processed with positive processing of 2 bar using Orochem Ezypress 48 (Spectralab, Ontario, Canada). The processing results in the entrapment of the free drug in the Superdex columns and this was eluted using multiple passages of 3.0 ml of buffer solution to determine the drug content (free drug). The entrapment efficiency was calculated using previously reported equations (18).

$$\text{Entrapment efficiency} = \frac{\text{(Assay of drugs- free drug content)}}{\text{Assay of drug}} \times 100$$

Importantly, formulations prepared for various OFAT studies having minimum entrapment efficiency ≥ 80% for both drugs were evaluated for the cryo-TEM and drug release.

7.2.4 Particle size and zeta potential

The hydrodynamic diameter, polydispersity index and surface potential were measured using quasi-elastic light scattering (QELS) using Zetasizer Nano ZS (Malvern Instruments Ltd., Malvern, UK) equipped with DTS software version 7.11 as described earlier. The particle size was determined using helium neon laser source of 633nm at light scattering angle of 175˚. The samples were diluted to appropriate concentrations (100 times) using 300 mM sucrose solution prior to analysis and intensity mode distribution of nanocarriers were recorded (19). The particle size was measured using translational diffusion coefficient by using the Stokes-Einstein equation

$$d(H) = kT/ 3\eta\pi D$$

where d(H) = hydrodynamic diameter; D = translational diffusion coefficient; k = Boltzmann's constant; T = absolute temperature, η = viscosity

The values of electrophoretic mobility (surface potential in mV) at surface of slipping plane were measured with undiluted samples and Smoluchowski equation using disposable electrophoretic folded cells. All measurements were performed in triplicate (20).

7.2.5 Cryogenic-transmission electron microscopy (cryo-TEM)

Morphological evaluation of various nanoliposomal formulations was done using cryo-TEM (TECNAI G2SBT, FEI, Eindhoven, Netherlands) with operation conditions of 200 kV and resolution of 0.27 nanometres. Glow discharger unit (Emitech K100X, Quorum Technologies ltd, England.) was used for the conversion of hydrophobic grid to hydrophilic one prior to application of the samples with subsequent vitrification at -180°C using liquid ethane (Vitrobot, FEI, Eindhoven, Netherlands). The samples were then included in grid holder with temperature being maintained using liquid nitrogen at -175°C and electron bombardment of 250 - 300 electron/nm^2 for 1 second exposure time. The morphology of the samples were

evaluated at a magnification of 70000X and 120 KV accelerating voltage with image processing with TECNAI software (18).

7.2.6 Drug release and release kinetics

The in-vitro DOX and VCR release from dual drug formulations was estimated at 37°±0.5 °C using molecular weight cut off device, Float-A-Lyzer G2 (Spectrum, New Jersey, USA). Briefly, 5 ml of nanoliposomal formulations were filled in the dialysis device and suspended in drug release medium (250 ml) of PBS (phosphate buffer saline) pH 7.4 and pH 5.5 under continuous stirring (150 rpm, Thermofisher Scientific, USA) (21). Sampling (1 ml) was done at 1,2,4,6, 12 and 24 hours with sampled volume being replaced with fresh medium at every time point. The collected samples were analysed for drug content as mentioned under section 2.3. The drug release studies were performed in triplicate with results being plotted as cumulative drug release ± standard deviation at each sampling time point (18). The drug release was model fitted for evaluation of mechanism of drug release. Higuchi model, Hixon-crowell model, zero order, Korsmeyer-Peppas model, first-order kinetic models were evaluated for determination of regression coefficients (22).

7.2.7 Physical form of DOX in liposomes

The physical form of the DOX (free HCl salt or aggregated sulphate) in the liposomal formulations with varying concentrations of ammonium sulphate were evaluated using UV absorption spectroscopy according to the previously described method (15). Briefly, the absorbance of different concentrations of DOX HCl in 10% w/v sucrose were taken at two different wavelengths of 470 nm and 550 nm using CARY 100 BIO UV-visible spectrophotometer (Agilent, California, USA). The absorption ratio (A470/A550) was then calculated for the various liposomal formulations with 10% w/v sucrose being used as a blank. The effect of concentration on the absorbance ratio of these wavelengths was established using the calibration curve of the free drug solution as reported earlier (15).

7.2.8 Factorial design

Post evaluation of the important CMA and CPP using the OFAT studies, further optimization of the entrapment efficiency, particle size and zeta potential was done using the full factorial design of experiments. The identified dependant variables such as lipid molar ratio, molar concentration of ammonium sulphate and pH of active drug loading were evaluated for identification of their impact on the CQAs while keeping the other variables constant during manufacturing of drug product. The nano-liposomal formulations were prepared using the method described under the section 7.2.2 with multivariate effect analysis using Minitab 17.3.1 (Minitab Inc, Pennsylvania, USA). Randomization of the experimental sequence was done with subsequent regression analysis as well as contour plots generation. The experimental validation of the multivariate model was done as compared to the predicted values.

7.2.9 Statistics

The statistical determination of level of significance ($p < 0.05$ considered significant) was done using Student's t-test and analysis of variance (ANOVA) (GraphPad Prism 6.0, USA)

7.3 Results and Discussion

The nanoliposomal formulations were prepared using ethanolic injection method and actively loaded with two amphipathic drugs DOX and VCR. The choice of liposome formation method presented advantage of higher volume of internal aqueous compartment along with ease of manufacturing and scalability (18). In current study, since active loading of both amphipathic drugs in same preformed nanoliposome were intended, availability of increased captured aqueous volume presented improved chances of drug encapsulation. Further, the colloidal nanocarrier should be presented with tailored physicochemical properties such as particle diameter, surface potential, stability and encapsulation efficiency to have desired pharmacokinetic-pharmacodynamic profiles post administration. Intravenous delivery of liposomes with hydrodynamic size $\leq$ 130 nanometres have been clinically found to have presented improved efficacy due to EPR (enhanced permeation and retention) mediated passive dissemination of the nanocarriers from leaky vasculature to target organs (23). Additionally,

nanoliposomes have presented lesser clearance and improved controlled release profiles when tuned to particle sizes of 30-200 nm respectively (24). Consequently, nanoliposomes with size of 50-200 nm present suitable opportunities for the high drug loading and efficient delivery (25). The levels of opsonization of the nanoliposomes have often been modulated by engineering the surface of the lipophilic membranes with hydrophilic components and imparting surface charges. Surface PEGylation with hydrophilic mpeg-2k-DSPE have presented negative surface charge with long circulation stealth properties to clinically approved nanocarriers improving their therapeutic efficiency while minimizing their toxicity (26). Since, OFAT based initial screening of the factors affecting the co-active loading of two drugs were intended in the present study, the chemical composition of USFDA approved liposomal Doxorubicin (DOXIL™) was taken as the base composition (23). The effect of change in responses were then evaluated by varying the independent CPP and the CMA of the process.

7.3.1 Phosphatidyl Choline chain length

The bilayer forming phosphatidylcholine (PC) components were evaluated for impact on the drug encapsulation efficiencies, particle size and zeta potential by varying the acyl chain length, membrane packing parameter and their lipophilicity. Longer chain fatty acids have been shown be associated with higher cellular uptake and drug retention while having varied effect on cellular viability (27). While DOX has been reported to be stably loaded in liposomes, VCR has been reported to exhibit leakage potential on storage (28). Consequently, varying the PC chain length may present changes in the encapsulation efficiency of VCR. The results of dual drug loading are presented in Table 16. The encapsulation efficiency of DOX was found to be high (>90%) with all the tested PCs while the VCR loading was found to increase with the increase in the chain length of the fatty acid. The liposomes prepared with HSPC and DAPC were found to present higher drug loading efficiencies (>80%) for both the drugs The increased temperature of drug loading (normally carried out at temperatures above T_g) results in bilayer hydrocarbon chains being transformed from ordered closely packed extended hydrocarbons chains into disordered liquid crystalline randomly oriented hydrocarbon chains with reduced

surface density (29). Factors affecting the phase transition temperature include the degree of unsaturation of the lipid, hydrocarbon chain length, type of headgroup and charge on it. When the molar ratio of the lipids is kept constant, variation in the fatty acid chain length of PC results in the difference in degree of Van der Waal's hydrocarbon's interactions and the energy required for disruption in the orderliness of the lipid bilayer. Long chain fatty acids have been associated with improved drug loading, stability and optimal drug release. This may be responsible for the improved encapsulation efficiency of the two drugs with HSPC and DAPC as the PC components. Further, the particle size of the different PC formulations was found to vary from 95 to103 nm while the zeta potential was found to vary from 1.57± 1.78 mV (DMPC) to -8.13 ± 1.88 mV (HSPC). The similar particle size of these formulations may be due to size reduction at temperatures above the Tm (same as that used for the drug loading). The decrease in the zeta potential with lower PC chain length may be due to decreased loading efficiency of the two drugs with higher free drug content of VCR in the liposomes (30). The release profiles of both the drugs were evaluated at pH 7.4 and 5.5 (Figure 26 A-B). The release profiles of the drugs from both the formulations T4 and T5 showed similar release profiles when tested at pH 7.4 and were similar to those reported earlier indicating low release of the drugs in the normal tissues as well as in blood during transit to the tumor cells over 24 hours period (16, 17). However, the DOX release profile of these two formulations when tested at pH 5.5 were significantly different with cumulative release of 54.31±3.81 % (HSPC liposome) and 28.85± 3.45% (DAPC liposome) being observed. Similar difference in results were observed with the VCR release from these formulations at pH 5.5. The decreased profiles of drug release from DAPC liposomes may be due to increased packing parameter as well as hydrophobicity associated with higher fatty acid chain length requiring higher time for hydrolysis of lipid bilayer and subsequent release of the drugs (31). The DOX and VCR drug release from both the formulations showed mixture of time-based diffusion (Higuchi) and erosion (Korsmeyer-Peppas) from the liposomes. Further, VCR release profiles indicated initial first order release prior to diffusion and erosion-based release. These results were similar to earlier reported release profiles (32). The morphological evaluation of the HSPC and DAPC liposomes were carried out using cryo-TEM (Figure 26 C-D). The formulations showed unilamellar

homogenous coffee bean shaped particles similar to that observed in case of clinically approved Doxil™. Since, the DAPC liposomes had significantly slower DOX release profiles as compared to clinical standard Doxil™, the intended release profile of the DOX from dual loaded liposomes for temporospatial presence with VCR at tumor site may get affected (15). Hence, HSPC was selected as phosphatidylcholine lipid bilayer forming component for further studies.

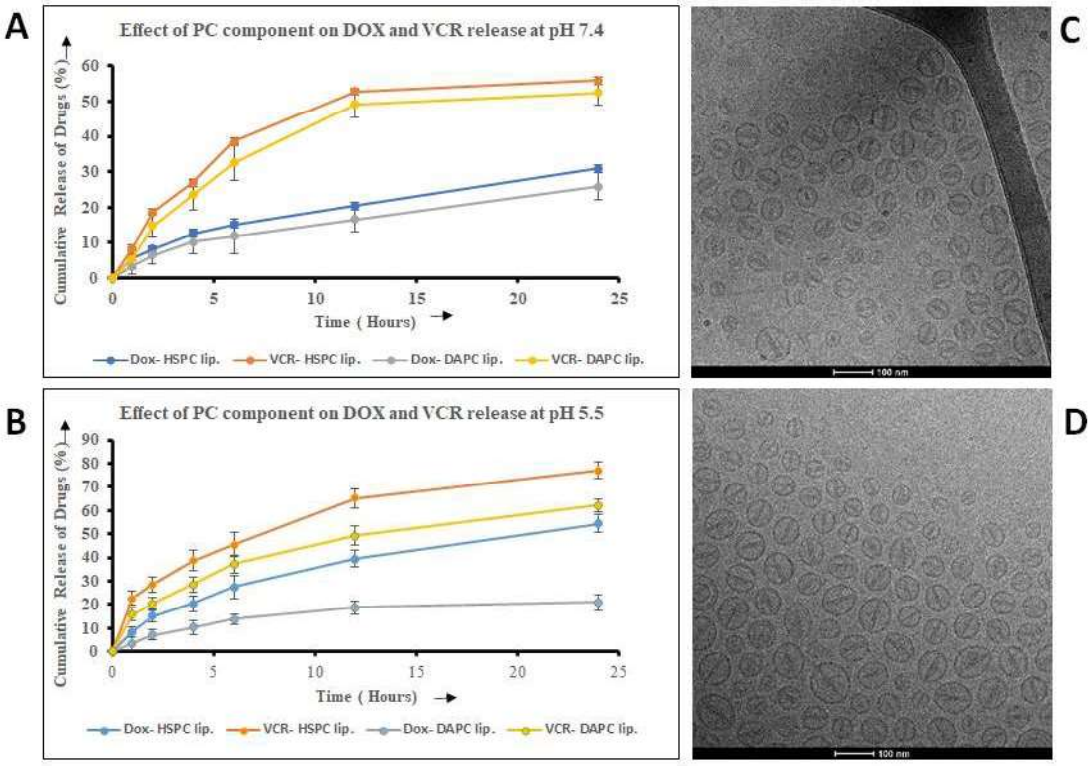

Figure 26: Effect of the variation in the Phosphatidylcholine chain length (HSPC and DAPC liposomes): on the drug release profiles at (A) pH 7.4 (B) pH 5.5; the cryo-TEM images of HSPC liposomes (C) and DAPC liposomes (D).

Variable	Batch code	Constant Independent factor	Variable Independent factor values	Assay-DOX (%)	FD-DOX (%)	EE-DOX (%)	Assay-VCR (%)	FD-VCR (%)	EE-VCR (%)	P.Size (nm)	PDI	Z.Potential (mV)
Phosphatidyl Choline chain length	T1	Conc. of Ammonium Sulphate: 250 mM; Lipid molar ratio (PC: Cholesterol:mpeg-2k-DSPE): 56.55:38.19:5.26	14:0 PC (DMPC)- Loading temp: 35˚C	99.56± 1.23	8.97± 1.35	90.99± 1.83	98.72± 2.15	31.56± 6.75	68.03± 7.08	96.58± 1.81	0.121	1.57± 1.78
	T2		16:0 PC (DPPC) - Loading temp: 55˚C	100.21± 1.09	7.41± 0.76	92.61± 1.33	98.72± 1.31	26.52± 5.39	73.14± 5.55	98.41± 3.15	0.103	-1.85± 2.45
	T3		18:0 PC (DSPC)- Loading temp: 65˚C	99.56± 1.38	6.53± 0.51	93.44± 1.47	98.72± 1.65	20.13± 4.76	79.61± 5.04	95.62± 1.23	0.091	-3.84± 3.81
	T4		18:0 PC (HSPC)- Loading temp: 65˚C	98.24± 1.51	2.58± 0.25	97.37± 1.53	97.61± 1.45	13.57± 2.52	86.10± 2.91	94.98 ± 3.19	0.075	-8.42 ± 2.67
	T5		20:4 PC (DAPC)-Loading temp: 75˚C	99.56± 0.69	8.97± 0.58	90.99± 0.80	98.72± 1.15	15.51± 3.56	84.29± 3.74	102.74 ± 1.98	0.151	-5.41±2.13
Transmembrane salt gradient	T4	Lipid molar ratio HSPC:Cholesterol: mpeg-2k-DSPE-56.55:38.19:5.26; Loading temperature: 65˚C	Ammonium sulphate (250 mM)	98.24± 1.51	2.58± 0.25	97.37± 1.53	97.61± 1.45	13.57± 2.52	86.10± 2.91	94.98 ± 3.19	0.075	-8.42 ± 2.67
	T6		Ammonium phosphate (250 mM)	100.19± 1.85	12.85± 2.65	87.17± 3.23	98.24± 3.25	25.45± 2.97	74.09± 4.40	95.89± 3.21	0.088	-2.68± 1.09
	T7		Ammonium Citrate (300 mM)	97.81± 2.39	10.59± 1.85	89.17± 3.02	97.13± 4.68	30.18± 4.56	68.93± 6.53	99.86± 6.18	0.133	-1.46± 2.47
	T8		Sulphobutylether Beta-Cyclodextrin ammonium salt (300 mM)	98.55± 2.91	15.68± 4.19	84.09± 5.10	99.28± 1.31	41.25± 5.35	58.45± 5.51	103.62± 1.23	0.127	1.18 ± 3.34
	T9		Copper sulphate (250 mM)	100.82± 3.55	21.57± 5.39	78.61± 6.45	98.31± 3.69	24.36± 3.37	75.22± 4.97	110.58± 5.81	0.109	-1.89 ± 2.67
	T10		Copper gluconate (250 mM)	101.51± 2.95	35.41± 6.98	65.12± 7.58	100.57± 3.44	50.65± 10.61	49.64± 11.15	105.36± 7.15	0.129	8.98 ± 3.56
	T11		EDTA Ammonium salt (250 mM)	103.22± 3.05	18.36± 3.59	82.21± 4.71	102.31± 2.15	28.81± 3.75	71.84± 4.32	107.15± 4.23	0.13	-2.16 ± 2.35
Drug loading temperature	T12	Conc. of Ammonium Sulphate: 250 mM; Lipids-	45˚C	98.31± 1.77	42.35± 4.89	55.96± 5.20	98.72± 2.63	48.56± 6.33	51.16± 6.85	103.75± 7.81	0.155	5.52± 1.89

Variable	Batch code	Constant Independent factor	Variable Independent factor values	Assay-DOX (%)	FD-DOX (%)	EE-DOX (%)	Assay-VCR (%)	FD-VCR (%)	EE-VCR (%)	P.Size (nm)	PDI	Z.Potential (mV)
	T13	HSPC: cholesterol: mpeg-2k-DSPE (molar ratio: 56.55:38.19:5.26)	55˚C	101.65± 2.05	10.71± 2.29	89.46± 3.06	100.31± 3.26	20.31± 5.49	79.75± 6.38	100.43± 3.82	0.141	-3.77± 1.52
	T4		65˚C	98.24± 1.51	2.58± 0.25	97.37± 1.53	97.61± 1.45	13.57± 2.52	86.10± 2.91	94.98 ± 3.19	0.075	-8.42 ± 2.67
	T14		75˚C	95.31± 4.59	4.21± 1.15	91.10± 4.73	94.21± 3.96	15.18± 3.35	79.03± 5.19	99.86± 6.18	0.133	-5.46± 2.47
Concentration of Cholesterol (lipid molar ratio)	T15	Conc. of Ammonium Sulphate: 250 mM; Lipids-HSPC: cholesterol: mpeg-2k-DSPE (molar ratios); Loading temperature: 65˚C	95.0:0.0:5.0	99.51± 3.63	40.57± 5.68	59.23± 6.74	98.72± 2.69	38.69± 3.55	60.42± 4.45	91.87± 3.77	0.254	5.67 ± 1.25
	T16		85.0:10.0:5.0	100.21± 3.59	25.08± 3.89	74.97± 5.29	99.61± 2.33	40.21± 5.69	59.63± 6.15	93.35± 2.69	0.158	3.74± 1.87
	T17		75.0:20.0:5.0	98.36± 3.78	15.41± 4.58	84.33± 5.94	101.13± 2.73	20.13± 3.19	80.09± 4.19	97.33± 3.59	0.121	-6.43 ± 1.69
	T4		56.55:38.19:5.26	98.24± 1.51	2.58± 0.25	97.37± 1.53	97.61± 1.45	13.57± 2.52	86.10± 2.91	94.98 ± 3.19	0.075	-8.42 ± 2.67
	T18		50.0:45.0:5.0	100.76± 2.39	5.42± 1.39	94.62± 2.76	98.69± 3.55	12.88± 3.86	86.95± 5.24	96.71± 4.85	0.075	-8.17 ± 1.96
	T19		40.65: 54.35:5.0	99.71± 2.15	6.68± 1.26	93.30± 2.49	100.45± 2.58	12.18± 3.35	87.87± 4.23	104.85± 1.39	0.134	-8.61 ± 1.68
Sequence of addition of drugs	T20	Conc. of Ammonium Sulphate: 250 mM; Lipids-HSPC: cholesterol: mpeg-2k-DSPE (molar ratio: 56.55:38.19:5.26); Loading temperature: 65˚C	1- DOX + 2-VCR as solution	99.58± 1.15	3.69± 0.71	96.29± 1.35	98.62± 2.88	16.21± 1.38	83.56± 3.19	98.54 ± 2.96	0.129	-7.19 ± 1.58
	T21		1- VCR + 2-DOX as solution	101.67± 2.49	4.41± 1.03	95.66± 2.69	99.41± 2.63	15.46± 2.46	84.45± 3.60	95.41 ± 3.68	0.095	-7.75 ± 1.95
	T4		DOX+VCR as solution	98.24± 1.51	2.58± 0.25	97.37± 1.53	97.61± 1.45	13.57± 2.52	86.10± 2.91	94.98 ± 3.19	0.075	-8.42 ± 2.67
	T22		DOX+VCR as powder	97.61± 2.63	4.12± 0.89	95.78± 2.78	99.31± 2.38	15.19± 2.68	84.70± 3.58	100.81± 3.56	0.058	-8.56 ± 1.19
pH of drug loading	T23	Conc. of Ammonium Sulphate: 250 mM; Lipids-	5.5	98.24± 1.51	2.58± 0.25	97.37± 1.53	97.61± 1.45	13.57± 2.52	86.10± 2.91	97.33 ± 2.65	0.069	-8.13 ± 1.88

Variable	Batch code	Constant Independent factor	Variable Independent factor values	Assay-DOX (%)	FD-DOX (%)	EE-DOX (%)	Assay-VCR (%)	FD-VCR (%)	EE-VCR (%)	P.Size (nm)	PDI	Z.Potential (mV)
	T4	HSPC: cholesterol: mpeg-2k-DSPE (molar ratio: 56.55:38.19:5.26); Loading temperature: 65˚C	6.5	100.51± 2.39	4.31± 1.36	95.71± 2.75	100.23± 2.69	12.86± 2.17	87.17± 3.46	94.98 ± 3.19	0.075	-8.42 ± 2.67
	T24		7.5	93.41± 3.48	20.51± 5.88	78.75± 6.83	99.31± 2.51	38.36± 4.59	60.95± 5.23	97.33 ± 2.65	0.069	4.84 ± 1.59
External medium	T4	Conc. of Ammonium Sulphate: 250 mM; Lipids-HSPC: cholesterol: mpeg-2k-DSPE (molar ratio: 56.55:38.19:5.26); Loading temperature: 65˚C	10% sucrose	98.24± 1.51	2.58± 0.25	97.37± 1.53	97.61± 1.45	13.57± 2.52	86.10± 2.91	94.98 ± 3.19	0.075	-8.42 ± 2.67
	T25		0.9 % saline	100.71± 2.53	10.31± 1.39	89.76± 2.89	101.23± 2.96	21.31± 3.68	78.95± 4.72	101.35 ± 4.69	0.130	-2.51 ± 1.88
	T26		5.0% Dextrose	99.15± 1.09	5.51± 1.46	94.40± 1.82	100.41± 2.76	15.76± 3.96	84.32± 4.83	98.33 ± 1.65	0.088	-5.06 ± 2.39
Drug to Lipid molar ratio	T4	Conc. of Ammonium Sulphate: 250 mM; Lipids-HSPC: cholesterol: mpeg-2k-DSPE (molar ratio: 56.55:38.19:5.26); Loading temperature: 65˚C	DOX- D:L= 0.16 VCR- D:L= 0.05	98.24± 1.51	2.58± 0.25	97.37± 1.53	97.61± 1.45	13.57± 2.52	86.10± 2.91	94.98 ± 3.19	0.075	-8.42 ± 2.67
	T27		DOX- D:L= 0.08 VCR- D:L= 0.025	97.68± 2.65	3.51± 1.26	94.17± 2.93	98.44± 2.16	12.98± 1.39	85.46± 2.58	96.41 ± 1.19	0.059	-8.13 ± 1.88
Concentration of Ammonium sulphate	T28	Lipids- HSPC: cholesterol: mpeg-2k-DSPE (molar ratio: 56.55:38.19:5.26); Loading temperature: 65˚C; External Medium: 10% Sucrose	150 mM	99.21± 1.67	35.87± 1.52	63.84± 2.26	99.31± 1.67	22.31± 1.95	77.53± 2.57	103.96 ± 2.19	0.139	-1.08 ± 1.83
	T4		250 mM	98.24± 1.51	2.58± 0.25	97.37± 1.53	97.61± 1.45	13.57± 2.52	86.10± 2.91	94.98 ± 3.19	0.075	-8.42 ± 2.67
	T29		350 mM	100.35± 1.78	3.81± 1.64	96.20± 2.42	102.71± 2.58	8.97± 1.56	91.27± 3.01	98.45 ± 3.35	0.081	-9.17 ± 1.19
	T30		450 mM	101.56± 2.36	7.81± 1.68	92.31± 2.89	98.47± 1.86	18.32± 3.53	81.44± 3.99	99.65 ± 3.51	0.103	-5.51 ± 1.39

* Abbreviations: DOX= Doxorubicin Hydrochloride; VCR= Vincristine sulphate; FD= Free drug; EE= Entrapment efficiency; PDI= Polydispersity index; Results of particle size and zeta potential are expressed as mean ± SD (n = 3).

Table 16: Results of dependent variables (entrapment efficiency of DOX and VCR; particle size and zeta potential) of formulations with the variation in independent variables based on one-factor-at-time (OFAT) studies

7.3.2 Transmembrane salt gradient

Transmembrane ion and pH gradient mediated active loading of the therapeutic agents in preformed liposomes have presented higher drug loading efficiencies suitable for clinical therapeutic usage (8). The results of the dual drug loading against various transmembrane salt gradients are presented in table 16. These results indicate that both drugs are simultaneously co-encapsulated to high values (97.37± 1.53% for DOX and 86.10± 2.91% for VCR) against ammonium sulphate gradient. While, the ammonium ion salts like ammonium citrate, ammonium phosphate, EDTA Ammonium and sulphobutylether β-Cyclodextrin ammonium salt showed > 80% loading for DOX, copper salts did not present good encapsulation efficiencies. The encapsulation efficiency of VCR was highest in case of ammonium sulphate while the other salts exhibited <76% loading of the agent. Importantly, the efficiency of remote loading of these agents shall depend on the physicochemical properties of the drugs such as dissociation constant pKa, permeability constant, ratio of charged to uncharged species at the loading pH and reaction kinetics with the "transmembrane pump" (5). The varying drug loading efficiency of the transmembrane ammonium salts may be attributed to the bilayer permeability coefficients of the charged counter-ions of these salts. Sulphate ion presents the lowest permeability and highest electrostatic potential for interaction with both the drugs. The drug loading mechanism in case of ammonium sulphate for both the drugs is presented in Figure 27. At the external drug loading pH of 5.5, both these weak amphipathic bases present higher levels of uncharged species allowing for the transmembrane transport of the drugs across the labile lipid bilayer at temperature above the T_m of the lipid composition (33). The presence of amino groups in indole ring of VCR and in daunosamine sugar in DOX present suitable functional group for the molecular interactions with the sulphate ion (Figure 27). Briefly, the entrapment of DOX and VCR in relation with ammonium sulphate is governed by transmembrane ammonium gradient and pH gradient generated when the drugs are loaded at a temperature higher than the T_m of the lipid composition. The heating of the liposomal suspension results in the increased concentration of the ammonium ion in inner aqueous layer, with subsequent diffusion of ammonia through liquid bilayer and protonation of inner layer

leading to increased acidic pH. Both the gradients are governed by the ratio of the ammonium ion in external medium and within the liposome. The protonated forms of the drugs DOX and VCR diffuse through bilayer and interact with the sulphate ion (having much lower permeation coefficient). The DOX and sulphate interaction leads to salting out of aqueous layer with accelerated flocculation and subsequent gelation with further increased uptake of the drug inside the liposomes. Further, the formation of the crystalline nanorods and subsequent precipitation of DOX sulphate in the inner aqueous compartment results in the shift of reaction kinetics towards the formation of the salt following Le Chatelier's principle (34). The DOX nanorod precipitate formation out of solution along with the interaction of VCR with sulphate ion resulting in formation of soluble salt may be responsible for the higher drug loading efficiency of DOX. The difference in the encapsulation efficiency of the drugs with other tested ammonium salts may be attributed to higher permeability of the counter ions through the disordered bilayer and increased solubility of the resultant drug salts being higher than that of sulphate salts at drug loading pH (4.0- 7.5) (8).

Copper salts were evaluated for drug loading as alternative to ammonium gradient. Two transmembrane gradients were evaluated: copper sulphate and copper gluconate/triethanolamine. Drug loading into the copper sulphate loaded liposomal suspension was found to be 78.61± 6.45% for DOX and 75.22± 4.97% for VCR whereas with copper gluconate they were found to be only 65.12± 7.58% and 49.64± 11.15% for DOX and VCR respectively. Copper being transition element with incomplete d-block element presents suitable opportunities for co-ordinate complexation and chelation with amino groups present in both the drugs. The lower drug loading capacity with copper sulphate may be attributed to lack of transmembrane gradient in absence of sufficient unionized groups for exchange in place of DOX and VCR. Post diffusion of the protonated forms, the low internal pH of the internal aqueous phase causes deprotonation of the drugs. These charged species have competing interaction possibilities with both copper and sulphate ions. The lack of suitable mechanism for the removal of either of the two species may have resulted in the collapse of the gradient and subsequent lower drug loading (35). The drug loading in case of copper gluconate gradient

has been attributed to the transport of the protonated drugs in exchange of the uncharged triethanolamine species at the drug loading pH (with absence of the any pH gradient) and subsequent complexation of the copper ions with the amino groups of the drugs (36). Since drug loading was carried at lower external pH of 5.5 against higher internal pH of 7.4, the ratio of uncharged to ionized triethanolamine species was lower (Triethanolamine pKa= 7.8) and may have attributed to the higher free drug contents (37).

The particle size of the formulations with ammonium salts of sulphate, citrate and phosphate ranged from 95 to 100 nm while the formulations with the other tested salts had higher size of 103 to 110 nm. Similar to results of the variation in PC component, the values of zeta potential were dependent on the levels of free drug content with range of -8.13 ± 1.88 mV (Ammonium sulphate) to 8.98 ± 3.56 (Copper gluconate/TEA).

The morphological evaluation of the dual drug loaded liposomes was done using cryo-TEM (Figure 28 A-G). The liposomes without any transmembrane salt exhibited showed spherical morphology without any internal precipitates/structures (Figure 28 A). Dual drug loaded liposomes with ammonium sulphate showed characteristic coffee bean shaped liposomes of DOX sulphate nanoprecipitates superimposed with electron dense VCR sulphate (Figure 28 B). Liposomal formulations with ammonium phosphate and citrate showed characteristic nanoprecipitates of DOX phosphate and needle shaped precipitates of DOX citrate respectively without any visible structures of VCR (Figure 28 C-D). Formulations with ammonium EDTA and ammonium sulphobutylether β-Cyclodextrin salts showed bilamellar and unilamellar morphology without any visible nanostructures in internal aqueous layer similar to the salt and drug free liposomes (Figure 28 E-F). Liposomal suspensions with copper salts showed electron dense internal aqueous compartment of copper complexes with DOX with additional nanoprecipitation of DOX sulphate in case of copper sulphate gradient (Figure 28 G-H). These results are in good correlation with earlier reported results (34, 38-40). Since, liposomal formulation prepared with ammonium sulphate showed high encapsulation efficiency (>86%) for both drugs, this salt was selected as transmembrane gradient.

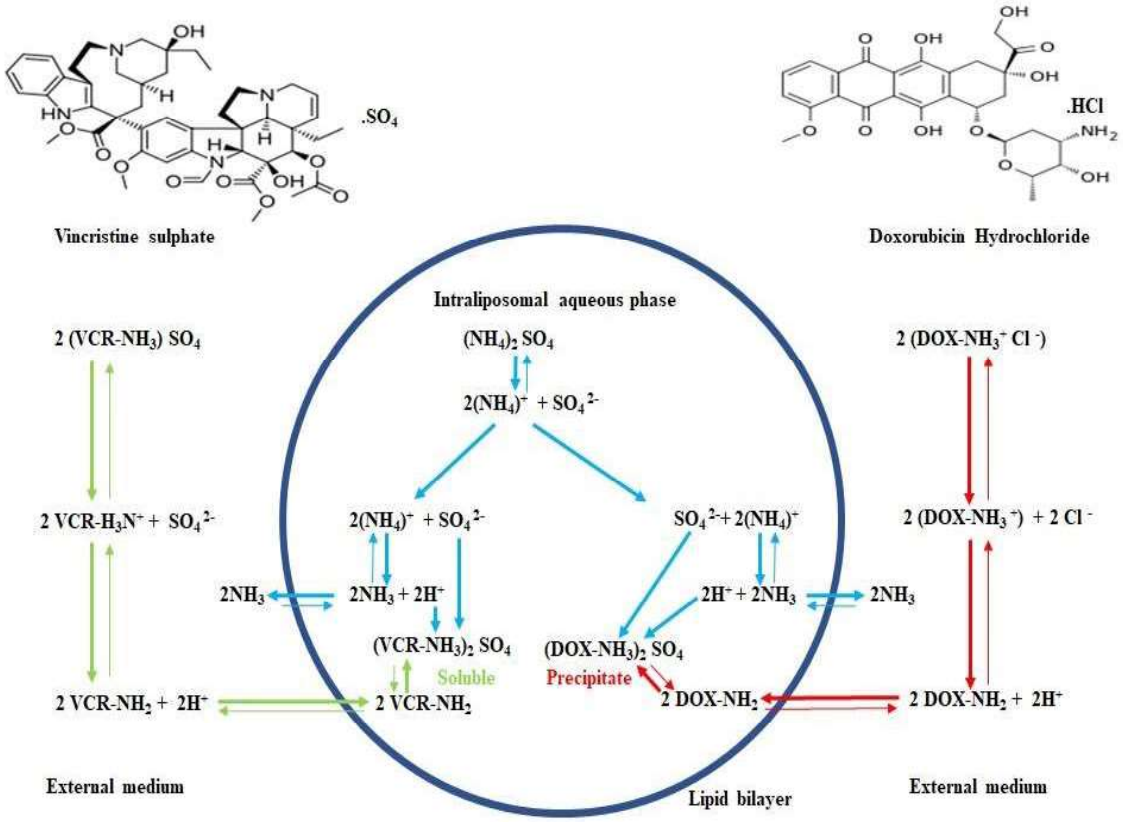

Figure 27: Schematic representation of the dual drug loading using ammonium sulphate transmembrane gradient.

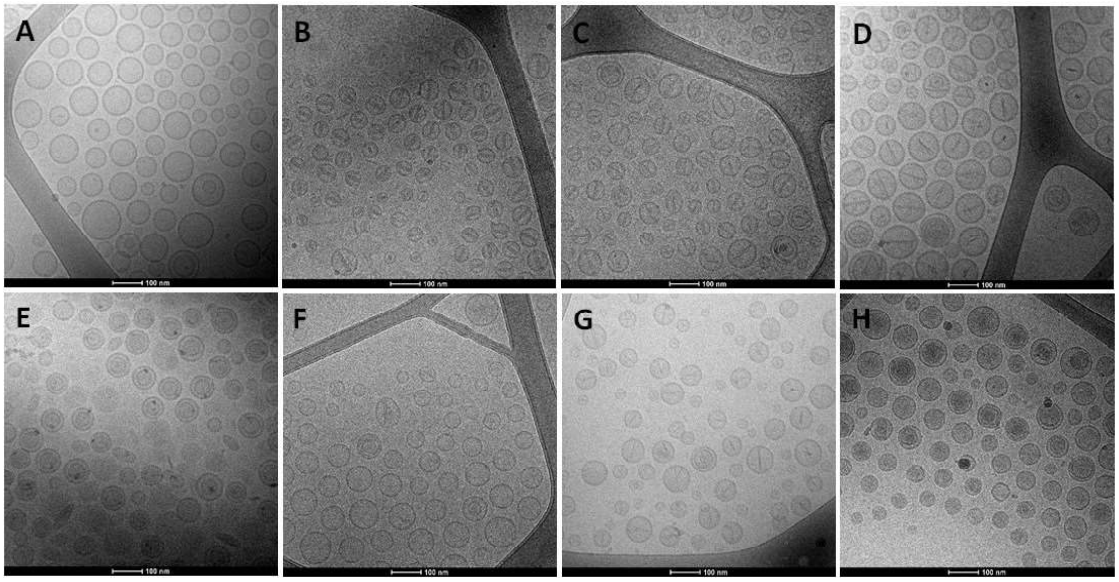

Figure 28: Cryo-TEM images of Pegylated liposomal suspensions of (A) Blank liposomes; Dual drug loaded containing different transmembrane salt gradients: (B) Ammonium Sulphate; (C) Ammonium Phosphate; (D) Ammonium citrate; (E) EDTA Ammonium salt; (F) Sulphobutylether Beta-Cyclodextrin ammonium salt; (G) Copper sulphate; (H) Copper gluconate/TEA

7.3.3 Drug loading temperature

Active drug loading of agents into preformed liposomes are carried out at elevated temperatures above the phase transition temperature (T_m). The T_m of PEGylate HSPC liposomes (56.55:38.19:5.26 mole ratio of HSPC: Cholesterol: mPEG-2k-DSPE) have been reported and experimentally found to be approximately 51 ± 2 °C (17, 41). The effect of drug loading temperature on the encapsulation efficiency of the two drugs were evaluated by loading the agents at 45°C,55 °C,65°C,75°C. The active loading of the drugs was found to show a temperature dependent decrease in free drug content with highest entrapment efficiencies at 65 °C (97.37± 1.53% for DOX and 86.10± 2.91% for VCR) (Table 16). These high loading values may be due to energy facilitated generation of sufficient bilayer disorderliness and creation of the transmembrane ammonium ion gradient. While the different drug loading temperatures

showed a variation in the degree of homogeneity of the particles (PDI) with active loading at 65°C exhibiting uniformity in particle size distribution (PDI= 0.069), there was a non-significant change in the measured particle sizes. The zeta potential values were found to be modulated by the free drug content of the formulations with active loaded formulation at 65°C showing a value of -8.13 ± 1.88 mV. Further, the results indicate that at temperatures below the T_m (45°C), free drug content of the liposomes was high (42.35± 4.89% of DOX and 48.56± 6.33% of VCR) while showing positive zeta potential (5.52± 1.89 mV). The high values of free drug may be attributed to the reduced fluidity of the bilayer, resulting in reduced translocation of the ammonia and protonated amphipathic bases which is further responsible for the higher positive surface potential. Morphological evaluation of effect of the drug loading temperature (45, 65 and 75°C) showed temperature dependent increase in the formation of the DOX sulphate nanoprecipitates in the coffee-bean shaped nano-vehicles. The active loaded dual drug loaded liposomes showed spherical morphology with some nano-precipitated structures and majorly empty at 45°C (Figure 29 A: white arrows). Loading at 55°C presented coffee bean shaped structures with some distorted structures (Figure 29 B: black arrows) while that for 65°C, predominantly coffee-bean shaped structures were observed (Figure 29 C). When the agents were loaded at 75°C distended coffee bean shaped morphology was seen (Figure 29 D: red arrows) with some empty vesicles (Figure 29 D: white arrows). The presence of the empty vesicles when drug loading was done at 45°C may be attributed to lack of sufficient fluidization of the bilayer membrane. The presence of such structures at loading temperature of 75°C may be due to leakage of ammonium sulphate when heated at high temperatures and disoriented recovery of the bilayer after completion of the process (34). These results indicate that the optimal drug loading temperature with the tested composition would be 65°C and the same was used for further studies.

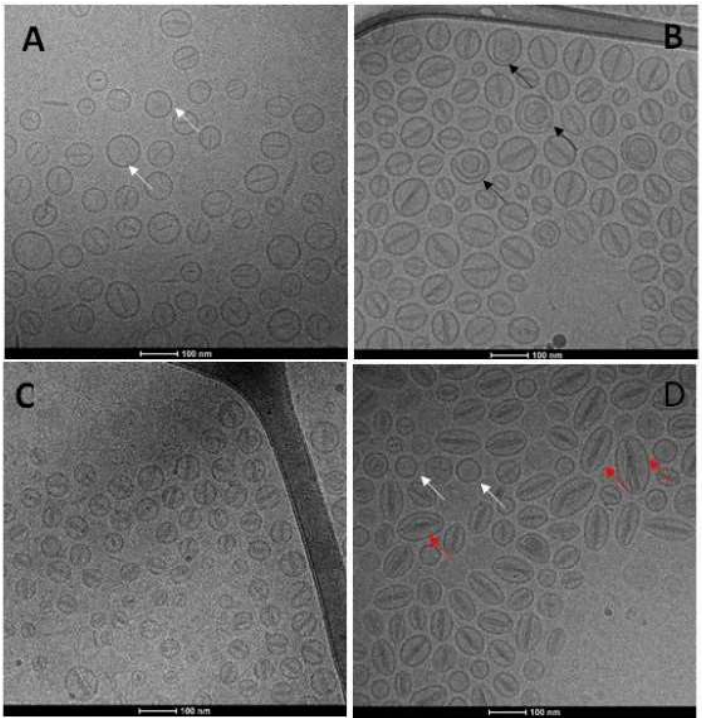

Figure 29: Cryo-TEM images of Pegylated liposomal suspensions with active dual drug loading at (A) 45°C; (B) 55°C; (C) 65°C; (D) 75°C.

7.3.4 Concentration of cholesterol (lipid molar ratio)

Since, no major improvements were observed in case of encapsulation efficiency of VCR and DOX with the change in PC component and transmembrane gradient, variation in molar concentration of cholesterol was tested. Traditionally, cholesterol has been added to liposomal formulations to provide the rigidity to the formed lipid bilayers. Cholesterol molecules have been reported to fill the gaps presented by the imperfect packing of hydrocarbon chains and have been associated with the membrane permeability, elasticity, stability, fluidity as well as modulation of drug release profiles (11). While the negatively charged polar hydroxyl group of cholesterol is aligned towards the external peri-liposomal and internal liposomal aqueous compartments, the remaining non-polar hydrocarbon rings are aligned as plugs between the PC hydrocarbon chains. The rigidifying agent have been included conventionally included at levels

of 20-45 mole % in clinically used liposomal formulations (Doxil™, Ambiosome™) except Vyxeos™ (containing 10% cholesterol) (42). The effect of addition of varying molar concentrations of cholesterol on the dependent responses were evaluated at levels of 0%, 10%, 20%, 38%, 45% and 55%. The results indicated a cholesterol concentration dependant increase in the entrapment efficiency of both drugs with optimal entrapment (>85%) being observed in case of 38%, 45% and 55% of cholesterol (Table 16). The active loading of liposomes formulated with 0% and 10% of cholesterol showed high levels of free drug of VCR and DOX which may be attributed to the lack of sufficient rigidity for retaining the drugs inside the preformed liposomes and the leakage potential of VCR from them (11, 43). The increased levels of cholesterol were found to improve homogeneity of the particles and non-significant increase in the particle hydrodynamic diameter similar to earlier reported values. The increase in the concentration of cholesterol was found to increase the zeta potential of the liposomes, with values of approximately – 8 mV for 38%, 45% and 55% moles of the lipid. The similar values of zeta potential of three formulations (T4, T18 and T19) may be due to improved encapsulation and reduced leakage of the drugs owing to cholesterol mediated efficient plugging of the imperfections in the bilayer (34). Drug loaded cholesterol free liposomes were found to have 5.67 ± 1.25 mV which may be due to high concentration of free drug owing to lack of cholesterol for rigidification of the formed liposomes. These liposomes exhibited distorted morphology (indicated by black arrows) along with majorly empty internal morphology (white arrows- Figure 30 A). The cryo-TEM images of the 38%, 45% and 55% moles of cholesterol showed the characteristic coffee bean shaped structures with uneven DOX distribution (indicated with white arrows) being observed in case of 38 mole% cholesterol (Figure 30 B-D). These three formulations were tested for in-vitro release at pH 7.4 and 5.5 (Figure 30 E-F). The release profile for DOX and VCR were similar in case of all these formulations when tested at pH 5.5 and pH 7.4. The release of the drugs at tumor pH (5.5) was found to approximately 50% for DOX and 71% for VCR after 24 hours. Similar to the previously studied in-vitro drug release profiles, both these drugs exhibited time-based diffusion (Higuchi) and erosion (Korsmeyer- Peppas) mixed kinetics from the tested liposomes. The significant difference in release profile of drugs from 55 mole% cholesterol

formulation as compared to the other two formulations may be due to the formation of localized cholesterol rich domains in the lipid bilayer having lesser packing parameter owing to less mole % of PC (44). Consequently, 38% and 45 mole % cholesterol were selected for evaluation during the further full factorial based formulation development and optimization. The ensuing OFAT studies were done with lipid composition with 38 mole % cholesterol.

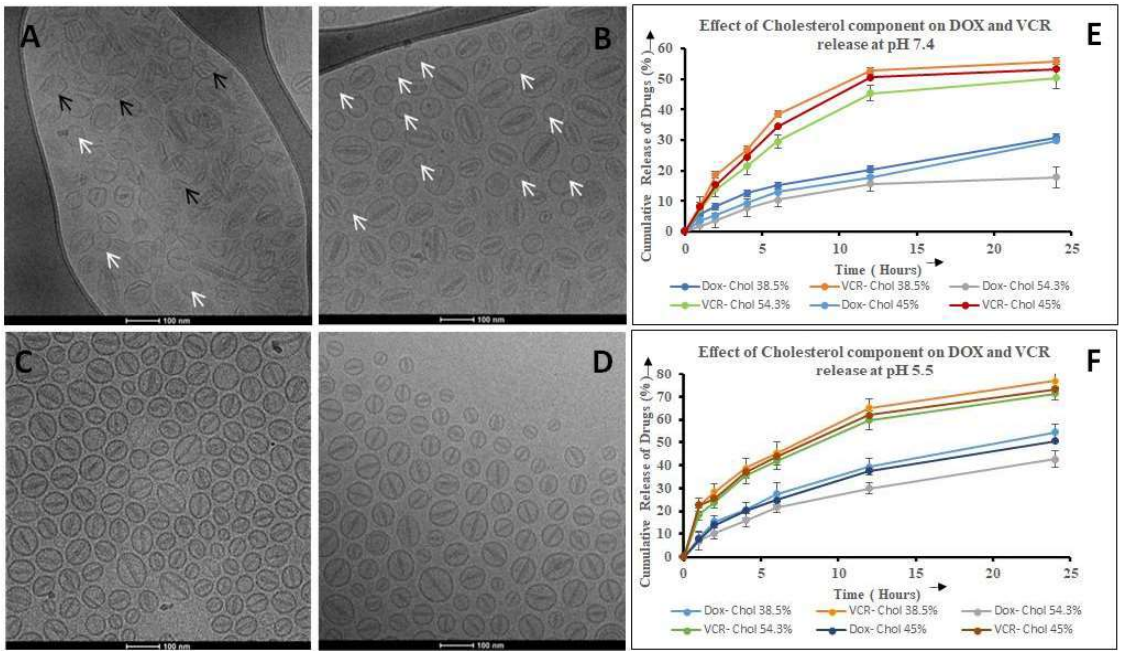

Figure 30: Cryo-TEM images of Pegylated liposomal suspensions with different molar concentrations of cholesterol in the lipid composition (A) 0 mole% cholesterol (B) 38 mole% cholesterol (C) 45 mole% cholesterol (D) 55 mole% cholesterol. Effect of variation in cholesterol content on the drug release profiles at (E) pH 7.4 (F) pH 5.5.

7.3.5 Sequence of addition of drugs

As evidenced from the previous OFAT studies, the DOX loading in preformed liposomes were found to be always higher than that of VCR. To evaluate the effect of the presence or absence of drug addition sequence during the active loading for a given ammonium sulphate

concentration, the drugs were added in the formulation in sequential and simultaneous manner. In the sequential loading (first DOX or first VCR), the two drugs were added to the heated liposomal suspension with a time gap of 15 minutes during incubation from the initial while for the simultaneous loading, both the drugs were added together. The results of the drug loading sequences showed 95-97% encapsulation efficiency for DOX while the values for VCR was found to be 83-86% only irrespective of the chronology of addition (Table 16). Simultaneous addition of DOX and VCR (dissolved in external medium) exhibited 97.37± 1.53% and 86.10± 2.91% encapsulation of DOX and VCR respectively. The observed higher values of loading of DOX as compared to VCR may be due to difference in reaction kinetics of formation of sulphate salts between the two protonated amphipathic bases post translocation of fluidized bilayer (Figure 27). The formation of DOX sulphate has been associated with salting out of aqueous layer, flocculation and nanoprecipitation with further increased uptake of the drug inside the liposomes. The DOX nanorod precipitate formation out of solution along with the interaction of VCR with sulphate ion resulting in formation of soluble salt may be responsible for the higher drug loading efficiency of DOX. Additionally, the lower intrinsic solubility of the DOX sulphate than VCR sulphate results in increased uptake of DOX inside the liposomes leading to lower DOX free drug levels (8). The sequence of loading of the drugs resulted in no significant changes in the particle size and zeta potential amongst the tested formulations with values ranging between 95.41 ± 3.68 nm to 100.81± 3.56 nm and -7.19 ± 1.58 mV to -8.56 ± 1.19 mV respectively. Based on these results, DOX and VCR were co-loaded simultaneously dissolved in external medium form for the subsequent studies.

7.3.6 pH of drug loading

The increased efficiency of the remote loading process using ammonium gradient has been observed for molecules having logD values from -2.5 to +2.0 and pKa≤11, with both VCR and DOX presenting the desired physicochemical properties (45). The presence of pH gradient facilitates the active drug loading using ammonium ion gradient. During the drug loading process when liposomes are heated and incubated with the drugs above the T_m, ammonia molecules migrate from the internal to external aqueous environment. The loading process has

been associated with two pH mediated events: the acidification of the internal layer due to residual H^+ ions and alkalization of the external medium with residual ammonia (Figure 27). The uncontrolled alkalinization of the external medium is prevented by buffering of the medium using histidine (46). This adjusted pH of drug loading of external medium was evaluated at pH 5.5, 6.5 and 7.5 to understand the effect of pH on the dependent responses. The encapsulation efficiency of DOX and VCR was found to be varying from 95.71± 2.75% to 97.37± 1.53% and 86.10± 2.91% to 87.17± 3.46% respectively when the drugs were loaded at pH 5.5 and 6.5 (Table 16). However, the entrapment efficiency was much lower in case of drug loading at pH 7.4 with values of 78.75± 6.83% and 60.95± 5.23% for DOX and VCR respectively. This variation in entrapment efficiency may be due to the change in the solubility of the protonated bases which decreases with the increase in the pH of external medium. Since, the ratio of surface area of non-polar to polar groups is higher for VCR than DOX, the pH mediated changes in the intrinsic solubility are higher for VCR. Conversely, DOX at lower pH presented in the internal aqueous environment has lesser solubility than VCR which further enhances the salting out of DOX sulphate. Additionally, with the pKa values of 8.68 (DOX) and 7.64 (VCR), the ratio of the charged to uncharged species would be higher at lower pH (5.5>6.5>7.5) allowing higher protonation of added drug salts at more acidic pH leading to increased transport across the fluid bilayer (47). Further, both VCR and DOX have been reported to have higher degradation profiles at pH 7.5 than the other tested acidic pH. The variation in drug loading pH had no significant impact on the particle diameter of the formulations while there was a significant change in the tested zeta potential at pH 7.4 than at other pH which may be attributed to the high levels of free drug present at the same pH (41). The drug release profile from T4 and T23 indicated that a non-significant difference exists between the drug release profiles from both these formulations when tested for release at pH 5.5 and 7.4 (Figure 31 A-B). Additionally, both these formulations did not exhibit any morphological differences and showed the coffee bean shaped structure with DOX nano-precipitation (Figure 31 C-D). Consequently, the active drug loading at pH 5.5 and 6.5 were selected for further evaluation during the full factorial-based formulation development and optimization. The ensuing OFAT studies were done with loading at pH of 5.5.

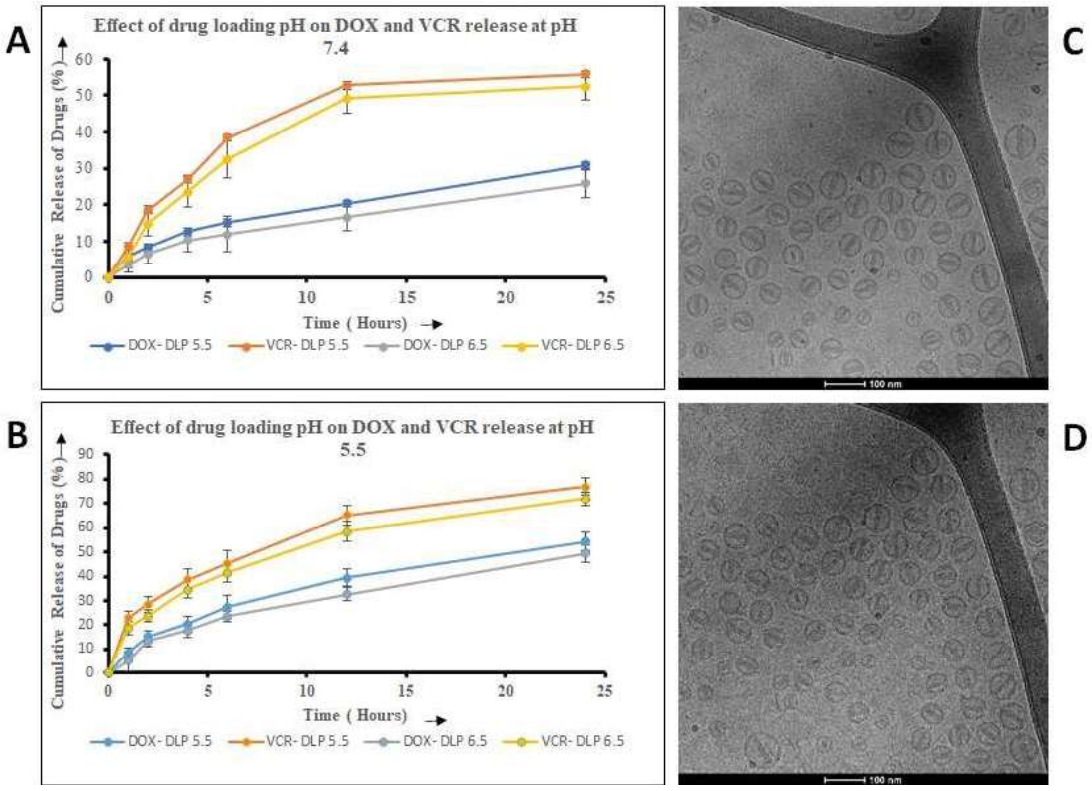

Figure 31: Effect of the variation in the drug loading pH (5.5 and 6.5): on the drug release profiles at (A) pH 7.4 (B) pH 5.5; the cryo-TEM images of dual drug formulations loaded at pH 5.5 (C) and pH 6.5 (D).

7.3.7 External medium

The external medium of the liposomal formulations has been normally taken as buffered non-electrolytes (sucrose/dextrose) and electrolytes (sodium chloride) which are iso-osmolar to both plasma and the aqueous environment inside the liposomes. Therefore, 0.9% saline, 5% dextrose and 10% sucrose were evaluated for the effect on the drug loading. The results indicate that the entrapment efficiency of DOX and VCR were in the order of sucrose>dextrose> saline (Table 16). This difference in the encapsulation of the drugs between the formulations may be explained as follows: PEGylated liposomes have been reported to have net negative charge and drug loading in presence of electrolytes may prevent the appropriate loading due to charge

screening of these liposomes. Further, the surface area ratio of non-polar to polar groups has been reported to be 1.20 (DOX) and 3.62 (VCR) indicating the presence of higher number of polar groups in DOX molecules (5). These groups present increased chances of electrostatic charged interactions with the electrolyte saline and may interfere with the protonation of the drug to uncharged species necessary for translocation across the membrane leading to reduced drug loading in comparison with non-electrolytes (Figure 27). Since VCR has lesser polar groups, the effect of electrolyte induced reduction in encapsulation efficiency was not profound in comparison with DOX. Additionally, the efficiency of ammonium sulphate transmembrane gradient for entrapment of the drugs inside the liposomes are governed by the ammonium ion concentration gradient and the pH gradient (Figure 27). The transport of ammonia to external medium results in increase in the pH which may result in the degradation of the drugs in case of absence of buffered external medium (saline). Additionally, the presence of sucrose in the peri-liposomal space near to the brush borders of the PEG chains presents steric hindrance to flocculation of the liposomes with prevention of aggregation leading to improved stability on storage as compared to the electrolyte (48). The presence of saline in the eternal medium resulted in poly-dispersed particle size distribution with reduced homogeneity as compared to the non-electrolyte external medium (49). The particle size distribution for the non-electrolyte external medium was found to be 94.98 ± 3.19 (10% sucrose) and 98.33 ± 1.65 (5% dextrose) while that for 0.9% saline was 101.35 ± 4.69. The zeta potential of the formulation with saline (-2.51 ± 1.88 mV) as external medium presented lower values than the non-electrolyte formulations (-8.42 ± 2.67 mV for sucrose/-5.06 ± 2.39 mV dextrose) which may be due to presence of increased counter ions in the volume of the slipping plane. Based on these results, sucrose buffered to pH 5.5 was selected for the subsequent studies.

7.3.8 Drug to lipid molar ratio

Another important factor which often affects the encapsulation efficiency of agents in liposomes during active loading process is the drug to lipid (D: L) molar ratio. The D:L ratio tested in the earlier OFAT studies was taken as that of the approved clinical formulation,

Pegylated Liposomal Doxorubicin (Doxil™) (D:L= 0.16). Since, the highest encapsulation efficiency of VCR in the co-loaded formulation (D:L= 0.05) was found to 86.10± 2.91% (T4), the drug to lipid ratio was reduced to evaluate the effect of the increase in the lipid content of the formulation. Increase in the lipid content often results in the increased number of lipid vesicles being formed based on the packing parameter of the lipid constituents (50). This increased number of liposomes leads to increased overall concentration of the transmembrane gradient in the formulations. However, the reduced D:L ratio (DOX:Lipid= 0.08 & VCR: Lipid= 0.025; increased lipid content) did not present any significant change in encapsulation efficiency, zeta potential and hydrodynamic diameter as compared to that of the higher D:L ratio (Table 16). However, these results may be attributed to the lack of appropriate transmembrane gradient for the active simultaneous loading of both the drugs despite an increase in the number of liposomes. Additionally, the higher intrinsic solubility of VCR sulphate than DOX results in the decreased translocation across the fluidized lipid bilayer in absence of required quantity of transmembrane gradient for both the drugs. These results are in good correlation with the earlier reported drug loading efficiencies and the D: L molar ratio for DOX and VCR were kept as 0.16 and 0.05 respectively for further studies (45).

7.3.9 Concentration of ammonium sulphate

Most of the aforementioned factors tested for their effect on the simultaneous encapsulation efficiency of both drugs showed no significant improvement was observed for the VCR loading. The concentration of the chosen transmembrane gradient ammonium sulphate was evaluated for the effect on the VCR loading. The results of the encapsulation efficiency studied against the varying concentration of the ammonium sulphate (150, 250, 350, 450 mM) indicate the concentration dependent improvement in the VCR loading till 350mM (Table 16). The encapsulation efficiency of DOX and VCR was found to be 96.20± 2.42% and 91.27± 3.01% respectively with 350 mM of ammonium sulphate (T29). The improved drug loading may be attributed to the availability of increased ammonium gradient for loading of the protonated

second amphipathic base (Figure 27). The lower solubility as well as precipitation of DOX sulphate at lower pH in internal aqueous environment results in maintenance of concentration gradient across the bilayer resulting in increased drug loading irrespective of the variations in the drug loading conditions (as indicated by the other OFAT studies). However, in case of VCR sulphate, the concentration gradient collapses once an equilibration is reached across both sides of the bilayer, resulting in less than 90% loading as well as subsequent leakage from the liposomes on storage (43). With two competing amphipathic bases for the existing 250mM and the intrinsic solubility profile of DOX, the presence of higher concentration of the gradient may have provided the additional transmembrane force for the loading of higher quantities of VCR in the liposomes. Further, the importance of ammonium sulphate transmembrane gradient was highlighted by the lack of loading of appropriate levels of DOX at 150 mM while being co-loaded with VCR. However, the formulation with 450 mM of ammonium sulphate exhibited reduced loading of VCR as compared to 350 mM and the reduction may be attributed to the decreased level of unionized species at high pH of external medium owing to increased release of ammonia. Further, with the ratio of surface area of non-polar to polar groups being higher for VCR than DOX, these pH mediated changes in the intrinsic solubility are higher of the drug (47). The variation in ammonium sulphate concentration showed no significant change on the hydrodynamic diameter of the liposomal formulations with uniform distribution of the liposomes (51). The presence of high amounts of free drug resulted in the formulations (150 mM and 450 mM) having reduced zeta potential while that in case of 250 mM and 350 mM presented increased surface potential values (-8.42 ± 2.67mV and -9.17 ± 1.19 respectively) owing to high drug loading efficiencies (Table 16) (30). Cryo-TEM based evaluation of T4, T29 and T30 showed no significant changes with all formulations having the spherical coffee bean shaped external morphology with DOX nanoprecipitation and presence of electron dense VCR sulphate (observed more in case of 350 mM) (Figure 32 A-C). The release profiles for DOX and VCR tested from the liposomes prepared with 250 mM and 350 mM ammonium sulphate presented non-significant difference between each other when tested at pH of normal tissues (pH 7.4) and inside tumor cells (pH 5.5) while exhibiting both diffusion and erosion controlled kinetic profiles (Figure 32 D-E).

The drug release from the liposomal formulation (Doxil™) has been reported to be slow from the sulphate nanoaggregates which along with the long circulation have been responsible for the Palmer-Plantar syndrome observed in patients receiving the formulation (52). Consequently, the increased concentration of ammonium sulphate presented higher chances of further reduction in the drug release kinetics. However, the increase in the concentration of ammonium sulphate was found to present non-significant change in the release profile of the drug. The physical form of DOX inside the liposome was evaluated to understand the possible reason of the similar release profile. The formation of DOX sulphate results in the shift of the absorbance of DOX from 470 nm (free HCl form) to 550 nm (sulphate aggregate form). The absorbance ratio (A_{470}/A_{550}) for both the formulations T4 (250 mM) and T29 (350 mM) was found to be 1.0945 and 1.0895 respectively. The results indicated that DOX was present in the formulations in aggregated form (at concentrations much higher than 1×10^{-3} moles of DOX inside the liposome) and level of aggregation was similar for both the formulations which may have been responsible for the similar in-vitro release profile. Based on the above results, the concentration of ammonium sulphate as transmembrane gradient was selected at 250 mM and 350 mM for further evaluation.

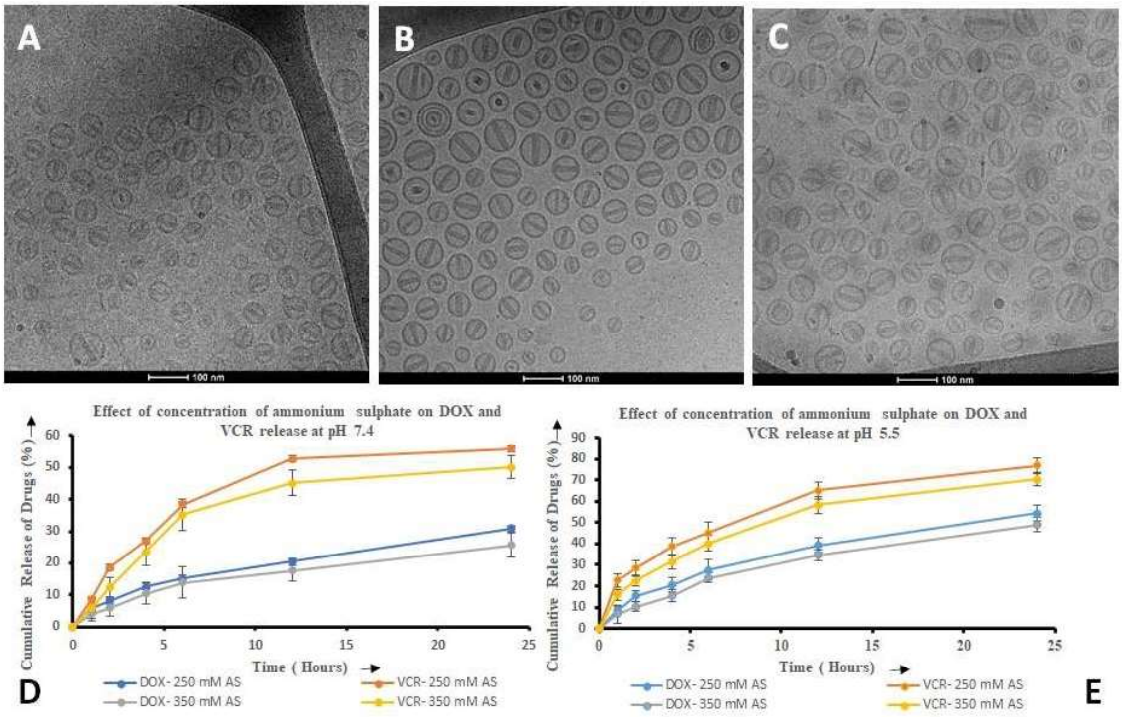

Figure 32: Effect of the variation in the ammonium sulphate concentration: cryo-TEM images- (A) 250 mM (B) 350 mM (C) 450 mM; drug release profiles at (D) pH 7.4 (E) pH 5.5. [Cryo-TEM image (B) has been reproduced with permission from (17)]

The aforementioned OFAT studies showed improved co-encapsulation efficiency of the drugs with optimal particle size and surface charge with variation in three independent variables: lipid molar ratio, pH of drug loading and molar concentration of ammonium sulphate. These variables were then varied simultaneously and further evaluated for their effect on the responses.

7.3.10 Factorial design

The OFAT studies presented three independent factors which affected the attainment of the desired quality target product profile (QTPP) of the dual drug loaded formulation. The preferred critical quality attributes (CQA) were set as encapsulation efficiency (>90% for both drugs), particle size (100±20 nm) and zeta potential (-10±2 mV) based on the CQAs of the

current clinical standard Doxil™ as well as the established requirements of intravenous drug delivery to tumor sites. The intended ethanolic injection method of liposomal suspension preparation exhibited various CMA and CPP. Based on prior literature and our experience of ethanolic injection method of liposomes preparation, critical parameters like rate of ethanolic injection, time of hydration, extrusion parameters and tangential flow filtration parameters were kept constant during the univariate and multivariate studies (15). The identified three dependant factors from the univariate studies were analysed further for their effect on dependent responses using multivariate full factorial 2^3 DOE. The results of the formulations prepared by the variation of these parameters are presented in Table 17. The significance of combination of three individual causal factors and corresponding interactions on the dependent outcomes were explored using regression analysis and ANOVA. This exploratory analysis was quantitively presented as polynomial interaction equation as previously described (16).

$$A_i = \alpha_0+\alpha_1B_1+\alpha_2B_2+\alpha_3B_3+\alpha_4B_1B_2+\alpha_5B_1B_3+\alpha_6B_2B_3$$

The regression equation indicated the changes in responses (A_i) like particle size, zeta potential and entrapment efficiency of the drugs effected by the individual/simultaneous variation of the independent factors (B_i, i=1 to 3) like concentration of ammonium sulphate, lipid molar ratio and pH of the drug loading. The multicollinearity coefficients of each factor on individual and simultaneous variation were indicated by α_i (i=1to 6) with α_0 being the regression constant/intercept on y-axis. The significance of the model equation and degree of fit were given by p-value, R^2 coefficient and F-value respectively. The coefficient of three factor variation presented lack of fit during interaction analysis and were subsequently removed during regression modelling. The qualitative estimation of the correlation efficiency was done using contour plots (Figure 33) while quantification was done using the regression equations.

7.3.11 Particle size

The efficiency of tumor passive targeting assisted through EPR phenomena is affected by the hydrodynamic diameter as one of the important surface design properties. The size related

extravasion and accumulation of the nanocarriers have been reported to be assisted through the leaky permeable vasculature, heterogenous nature of tumors as well as reduced lymphatic clearance (53). Additionally, the potential of plasma protein binding, phagocytic clearance, hepatic uptake and phenomenon of CARPA (complement activation-related pseudoallergy) have been shown to be dependent on the particle size of the nanoliposomes (54). The optimal particle size of the PEGylated liposomes for evasion of the components of MPS, reduced perfusion to unintended sites and improved systemic delivery of drug payload to tumor tissue has been reported to be 100±20 nm (55). Further, the particle size distribution has been reported to have significant impact on fate of the nanoliposomes during plasma transit and accumulation in unintended/intended sites leading to differences in therapeutic outcomes in relation to safety and efficacy. The polydispersity index (PDI) measured provides an indication about the parametric correlation variability of size distribution. The PDI values <0.1 have been found to present monodisperse homogenous populations for nanoliposomes as emphasized by the guidance of regulatory agencies USFDA and EMEA (56).

The average particle size of the nanoliposomes were determined using QELS principle with results being reported in Table 17. The highest and lowest particle size for the DOE based formulations was found to be that of DV2 (115.41±5.81 nm) and DV6 (95.74±2.65 nm) respectively. These results and regression equation indices indicate that increase in concentration of transmembrane gradient, decreased pH of drug loading and increased lipid molar ratio is associated with reduced values of Z-average. The interaction terms for two factor variations indicated a positive effect on the particle size with all multicollinearity coefficients indicating significant impact on the nanoliposomal size as indicated by the p-values the regression equations (Table 18). The qualitative correlation of causes with effect on particle size was further evaluated using contour plots (Figure 33 A-C).

Batch Code	Salt conc. (mM)	PC: Chol. ratio	Lipid molar ratio	Total lipid (mg/ml)	pH of drug loading	Assay DOX (%)	FD DOX (%)	EE DOX (%)	LE DOX (%)	Assay VCR (%)	FD VCR (%)	EE VCR (%)	LE VCR (%)	Particle size (nm)	PDI	ζ Potential (mV)
DV1	350	1.11	A	15.96	6.5	102.61±1.12	4.52 ±0.31	98.09±1.15	12.29±1.38	101.15±1.58	8.97±0.35	92.18±1.62	5.78± 0.86	110.32±2.35	0.133	-6.79±1.85
DV2	250	1.11	A	15.96	6.5	101.78 ±2.29	6.57± 1.29	95.21±1.87	11.93±1.45	102.86±1.67	14.81±1.98	88.05±1.41	5.52±0.63	115.41±5.81	0.071	-1.96±2.15
DV3	250	1.48	B	15.96	6.5	98.24 ±3.15	2.34± 0.89	95.90±2.48	12.02±1.58	98.67±1.37	13.57±1.75	85.10±1.67	5.33±0.74	104.21±3.65	0.056	-2.81±1.58
DV4	350	1.48	B	15.96	6.5	98.51 ±2.51	5.31± 1.59	93.20±3.61	11.68±1.35	98.45±1.58	7.51± 1.86	90.94±1.38	5.70±0.52	103.45±4.96	0.077	-7.86±1.79
DV5	250	1.11	A	15.96	5.5	101.41 ±1.25	5.53± 1.87	95.88±3.85	12.02±1.61	101.91±1.62	12.77±2.51	89.14±1.71	5.59±0.68	113.71±5.68	0.102	-3.57±2.98
DV6	350	1.48	B	15.96	5.5	100.35 ±1.49	1.48± 0.25	98.87±1.88	12.39±1.15	102.71±1.78	5.97± 0.63	96.74±1.85	6.06±0.25	95.74±2.65	0.069	-9.17±1.19
DV7	350	1.11	A	15.96	5.5	101.37 ±1.15	3.18± 1.19	98.19±1.95	12.30±1.54	100.47±1.59	6.25±0.86	94.22±1.53	5.90±0.35	108.35±5.96	0.141	-8.24±2.31
DV8	250	1.48	B	15.96	5.5	99.71 ±1.79	4.87± 2.51	94.84±2.12	11.88±1.76	98.81±1.92	11.51±2.19	87.30±1.36	5.47±0.71	101.23±3.64	0.081	-4.12±3.19
DV9[$]	350	1.48	B	15.96	5.5	-	-	-	-	-	-	-	-	93.32±3.67	0.083	-24.05 ±1.12
DV10[$]	350	1.48	B	15.96	5.5	102.41±1.67	2.78± 1.48	99.63±2.35	12.48±1.58	-	-	-	-	98.45±4.76	0.049	-12.50±1.25
DV11[$]	350	1.48	B	15.96	5.5	-	-	-	-	101.77±1.56	4.18± 1.21	97.59±1.69	6.12±0.85	96.29±4.41	0.065	-8.00±1.79

* Abbreviations: A/B= lipid molar ratio 50:45:5/56.55:38.19:5.26 (HSPC: Cholesterol: mpeg-2k-DSPE); Salt= Ammonium sulphate; DOX= Doxorubicin Hydrochloride; VCR= Vincristine sulphate; FD=Free drug; EE= Entrapment efficiency; LE=Loading efficiency; PDI= Polydispersity index;

[$] DV9, DV10 and DV11 are drug free, DOX liposome and VCR liposome respectively, prepared with the composition of the optimized formulation DV6; Results expressed as mean ± SD (n = 3).

Table 17: Results of entrapment efficiency, loading efficiency, particle size and zeta potential of formulations with the variation in factors based on Full factorial design

The plots indicated levels of the factors as 350 mM ammonium sulphate, drug loading at pH 5.5 and lipid ratio of 56.55:38.19:5.26 (HSPC: Cholesterol: mPEG-2k-DSPE) was found optimal for desired hydrodynamic diameter. The variation in the particle size may be due to changes in the pH induced lipid migration, polarization induced local heterogeneities in bilayer membranes, dynamic deformities as well as changes in the packing parameters during liposomal active drug loading (57). These results present good correlation with previously tested and model fitted active loading strategies for the drugs (5). The heterogeneity index of the distribution varied from 0.069 (DV6) to 0.141 (DV7) with D_{90} values of 150 nm and 196 nm respectively. The low values of SPAN and the PDI indicate unimodal monodispersed size distribution of the formulations with homogeneity synonymous to easier aseptic filtration and increased accumulation of the particles at the intended tumor lacunae. These results may be attributed to the built-in controls for attainment of desired particle size and its distribution during the manufacturing of the liposomes.

7.3.12 Zeta Potential

The cytotoxic potential of the nanoliposomes is often affected by the polarity as well as density of the electrostatic charge. Although, nanocarriers with surface potential in range of 0±30 mV has been considered to represent unstable colloids, presence of high positive charge has been reported to have issues related to toxicity, aggregation and adsorption in presence of plasma proteins as well as altered cellular uptake (58). Clinically, zeta potential of 0±10 mV has been found to present improved blood circulation time, reduction in the opsonization potential by MPS (mononuclear phagocyte system) and EPR mediated non-specific tumoral uptake (59). The slightly negative zeta potential of these liposomal formulations may be attributed to 5% molar concentration of mPEG-2k-DSPE and cholesterol (60). The DOE trials for the variation in the independent factors showed values of electrokinetic potential varying from -9.17 ±1.19 mV (DV6) to -1.96 ± 2.15 mV mV (DV2) (Table 17). The regression coefficients of the variables and contour plots are presented in Table 18 and Figure 33 respectively. The increase in the concentration of ammonium sulphate was found to have increased the values of the surface potential (DV6). The higher zeta potential values may be attributed to the decreased

values of free drugs DOX and VCR resulting in increased protonation of the amphipathic agents and improved uptake in the liposomes. Further, formulations prepared with 250 mM of ammonium sulphate was found to have presented higher deprotonated free drug content due to lack of sufficient transmembrane gradient with near neutral values of -1.96±2.15 mV (DV2). Similarly, the increase in the lipid molar ratio and decreased drug loading pH was found to present increased zeta potential values. These results may be further attributed to the mechanism of the drug loading against the trans-bilayer gradient and subsequent free drug content (Figure 33) (60). The values of interaction terms indicate negligible effect of simultaneous variation in the variables while the individual coefficients showed significant effect ($p<0.05$). Further, the results showed that variation in concentration of ammonium sulphate had a more profound effect on the surface potential values which may conceivably be due to effect on free drug content. The contour plots indicated the values of 350 mM ammonium sulphate, drug loading at pH 5.5 and lipid ratio of 56.55:38.19:5.26 (HSPC: Cholesterol: mPEG-2k-DSPE) for achieving the intended zeta potential (Figure 33 D-F). Formulation DV6 prepared with these levels of independent variables exhibited a zeta potential of -9.17±1.19 mV which was similar to that of clinically used liposomal Doxil™ and consequently the formulation may present suitable properties for delivery of the agents to tumor site (5).

7.3.13 Entrapment efficiency (EE) and morphology

The total and free DOX, VCR content were determined using RP-HPLC and GPC (gel-permeation chromatography). The optimal levels of entrapment of the drugs are important considering the therapeutic response afforded by the agents when present simultaneously in the same carrier (14). The efficient drug loading in the nanocarrier leads to optimal controlled delivery of the drugs and improved therapeutic efficiency (61). The results of these DOE trials (Table 17) presented the lowest levels of DOX and VCR encapsulation as 94.84±2.12 (DV8) and 85.10± 1.67% (DV3) respectively. The formulation DV6 exhibited the highest entrapment efficiencies with free drug levels of 1.48± 0.25% and 5.97± 0.63% for DOX and VCR

respectively. The regression coefficients of the individual and interaction variables are presented in Table 18. The regression equations for the encapsulation efficiency of DOX and VCR indicated that co-loading of the drugs was higher when concentration of ammonium sulphate was taken as 350 mM. Formulations prepared with 350 mM reported values of EE > 96.20±3.61 (DOX) and EE> 90.94±1.38% (VCR) in batch DV4. The concentration of ammonium sulphate was found to have positive effect on the loading of the drugs with increase in the EE with increased concentration of the transmembrane gradient. The effect of the salt gradient was higher in case of VCR than DOX. The positive increase in the EE of the drugs may be attributed to presence of higher transmembrane gradient for both the competing protonated amphipathic bases (Figure 27). The lower EE of VCR in presence of lower level of gradient salt may be due to higher intrinsic solubility of the drug in the lower pH of the internal aqueous compartment and equilibration associated collapse of the gradient for the drug.

Further, EE of drugs were higher when co-loaded at pH of 5.5 with increase in pH found to result in decrease in entrapment especially VCR. The higher EE may be due to higher protonation and higher intrinsic solubility of the drugs at lower pH leading to better transport across the lipid bilayer. Similarly, the increase in lipid concentration was found to result in decrease of the EE when the pH of the drug loading was higher (pH 6.5) and increased when the corresponding pH was lower. All the interaction terms for the simultaneous variation of all causal terms had a negative effect on the entrapment efficiency of the drugs (8). These variations had a significant impact on the drug loading as indicated by the p-values for both the regression equations. Subsequently, the correlation effect of variation in independent factors on the EE was measured using contour plots (Figure 33 G-L). These plots indicated levels of the factors as 350 mM ammonium sulphate, drug loading at pH 5.5 and lipid ratio of 56.55:38.19:5.26 (HSPC: Cholesterol: mPEG-2k-DSPE) were found optimal for suitable entrapment efficiency of both drugs. These results present good correlation with previously tested and model fitted active loading strategies for the drugs (5). Based on these DOE results, the parameters of nanoliposomal formulation DV6 was found to present the optimum values for the efficient co-loading of the drugs in single nanoliposome. Regression equations of all

the three responses were experimentally validated against theoretical values when tested at the optimal values of causal factors (DV6) (table 18). The experimental results presented non-significant differences with the theoretical values indicating the suitability of the regression models.

Morphological evaluation using cryo-TEM was performed for the formulations DV4, DV6, DV7 and DV8. These formulations did not exhibit any morphological differences and exhibited the characteristic coffee bean shaped structures with DOX nano-precipitation as well as electron-dense soluble VCR-sulphate (Figure 34 A-D). These formulations were further tested for their drug release profiles.

Parameter terms	**Parameter Description**	**Coefficient of the variable on Particle size**	**Coefficient of the variable on Zeta Potential**	**Coefficient of the variable on Entrapment efficiency- DOX**	**Coefficient of the variable on Entrapment efficiency- VCR**
b_0	Constant	106.928	-5.565	96.2725	90.4588
b_1	Ammonium sulphate Conc. (A)	-1.7125	-2.45	0.815	3.06125
b_2	PC: Cholesterol ratio (B)	-5.02	-0.425	-0.57	-0.43875
b_3	pH of Drug loading (C)	1.42	0.71	-0.6725	-1.39125
b_4	Interaction of Ammonium sulphate Conc. * PC: Cholesterol ratio (AB)	0.9	-0.075	-0.4825	0.75875
b_5	Interaction of Ammonium sulphate Conc. * PC: Cholesterol ratio (AC)	0.25	-0.02	-0.77	-0.56875
b_6	Interaction of PC: Cholesterol ratio* pH of drug loading (BC)	0.5025	-0.055	-0.48	-0.60875
R^2		0.9626	0.9962	0.9675	0.9309
F		156.50	279.11	49.99	85.49
p		<0.05	<0.05	<0.05	<0.05
Validation of the linear model using optimized formulation		**Particle size (nm)**	**Zeta Potential (mV)**	**% Entrapment efficiency-DOX**	**% Entrapment efficiency-VCR**
Predicted	Ammonium sulphate- 350 mM; PC: Cholesterol ratio- 1.48 pH of drug loading- 5.5	98.93	-9.15	97.96	96.40
Actual		98.74	-9.17	98.87	96.74

Table 18: Summary of Regression analysis and effect of Process variables on the tested responses of dual drug liposomes

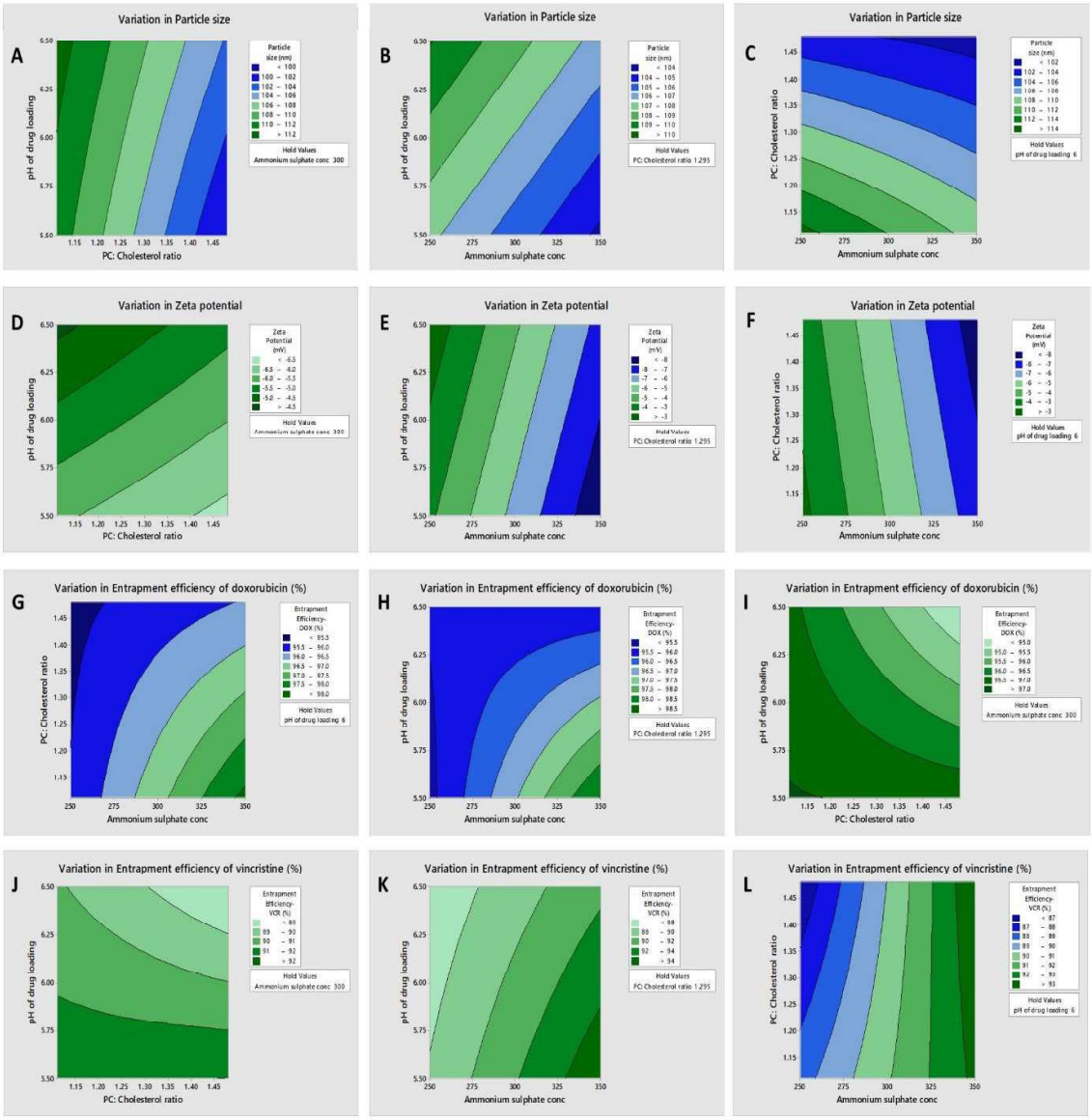

Figure 33: Contour plots of responses- Particle Size (A-C), Zeta potential (D-F), Entrapment efficiency of DOX (G-I) and Entrapment efficiency of VCR (J-L) as a measure of the factors (pH of drug loading, Ammonium sulphate concentration, PC: Cholesterol ratio) [Contour plots have been reproduced with permission from (16)].

7.3.14 Drug release and kinetics

The in-vitro release studies of DOX and VCR were tested at pH 7.4 and pH 5.5 to evaluate the effect of physiological conditions during plasma transit and after uptake in the cancerous cells post intravenous administration of the formulations. The formulations DV6, DV7, DV8 and DV4 were evaluated for the drug release. While DV6 presented the most optimal CQAs, the other formulations were taken as controls being prepared with variation in pH of drug loading (DV4), lipid molar ratio (DV7) and concentration of ammonium sulphate (DV8). The formulation DV8 presented formulation QTPP of VCR co-loading into the clinically used liposomal Doxorubicin hydrochloride (62). The in-vitro drug release profiles are presented in Figure 34 (E-H). The release of DOX and VCR was found to be pH dependent with increased cumulative release at lower pH (simulation of the pH conditions inside the tumor) having profiles similar as reported earlier (15, 63) . The drug release profiles at pH similar to that inside the tumor cells (pH 5.5) showed mixed release profiles. DOX release at this pH from was found to present a staggered release with $t_{50\%}$ values of 10.2 hours (DV4) to 24.54 hours (DV6) (Figure 34 E). VCR from formulations exhibited burst release (initial) followed by erosion based secondary release with $t_{50\%}$ release varying from 8.77 hours (DV4) to 10.32 hours (DV6) (Figure 34 G). The formulation DV6 presented a cumulative release of 48.89±3.54% DOX and 70.11±2.59% VCR over the tested time period (24 hours).

Additionally, DOX release at pH 7.4 (pH of normal tissues/blood) after 24 hours from all the formulations was found to be maximum for DV4 (31.63±1.68 %) and least for DV6 (23.55±1.55%) (Figure 34 F). The results of VCR release ($t_{50\%}$) at pH 7.4 from the nanoliposomes was found to range from 11 hours (DV4) to 27 hours (DV6) (Figure 34 H). These results of drug release at both pH presented good correlation with previously reported study results (64). Interestingly, the dual loaded formulation DV6 presented a similar DOX release profile to DV8, indicating that the release of DOX was unaffected by the presence of additional drug as well as increased concentration of ammonium sulphate. The formulation DV4 was found to present higher drug release profiles of both drugs when tested at pH 7.4 and 5.5 despite having ammonium sulphate concentration same as that of DV6 (formulation with

reduced release profile). The faster DOX and VCR release from nanoliposome may be attributed to difference in the levels of protonation of the amphipathic bases and subsequent difference in the sulphate salt formation as well as solubility constants (K_{sp}) in internal aqueous environment post diffusion through the bilayer (63).

These results indicated that the drug release from the dual loaded nanoliposome exhibited mixed kinetic profiles. DOX was found to present controlled release over the tested time period mediated through Fickinian diffusion (Higuchi model) along with erosion followed by diffusion mechanisms (Korsmeyer-Peppas). Such profile may be owing to the controlled rate of DOX release from the insoluble nanoprecipitate into the internal aqueous compartment followed by diffusion to outside the nanocarrier post erosion of the lipid bilayer (22). VCR was found to present biphasic release profiles explained by initial first order kinetic model followed by secondary phase governed by Higuchi as well as Korsemeyer-Peppas models. The initial release may be attributed to the higher intrinsic solubility of the VCR-sulphate in inner aqueous compartment along with higher transmembrane permeability across the bilayer. The secondary release may be explained by the diffusion of the drug in response to the erosion of the liposomal bilayer (63, 64). Importantly, all the tested formulations exhibited similar patterns of individual drug release, which were not affected by the co-presence of drugs indicating towards possible temporospatial presence of both drugs at the tumor site (3).

The optimal nanoliposomal formulation DV6 was further physico-chemically characterised to ascertain the differences between the dual loaded nanoliposome and clinical standard liposomal doxorubicin hydrochloride.

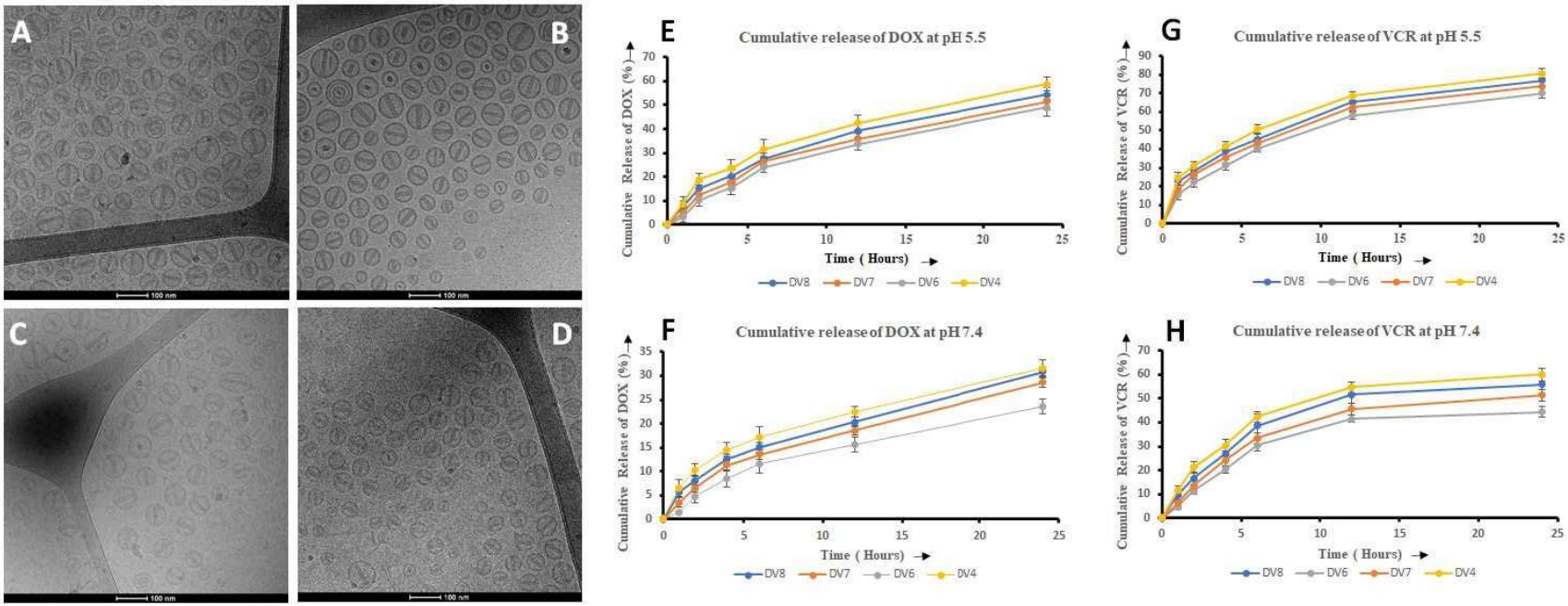

Figure 34: Morphological evaluation of DOE batches using Cryo-TEM: (A) DV4, (B) DV6, (C) DV7 and (D) DV8; in-vitro drug release profiles: cumulative release from formulations (E) DOX at pH 5.5, (F) DOX at pH 7.4, (G) VCR at pH 5.5, (F) VCR at pH 7.4. [Cryo-TEM image (B) has been reproduced with permission from (17)]

7.4 Conclusion

The current study was aimed at rationale-based design of dual drug loaded nanoliposomes having optimal physico-chemical properties such as adequate encapsulation efficiency, particle size, zeta potential, morphology and drug release for effective treatment. A systematic QbD approach was used for building in the intended QTPP by establishing a correlation between the dependent variables and the independent CMAs as well as CPPs. The approach was subdivided into two parts: univariate analysis for identification of important causal factors and multivariate DOE studies for identification of the optimized formulation. The PEGylated liposomes were prepared using ethanolic injection method while the drugs DOX and VCR were subsequently actively co-loaded in preformed single liposomes. Various CPP/CMA like transmembrane salt gradient, lipid-molar ratio, drug loading temperature, phosphatidylcholine chain length, sequence of drug addition, drug loading pH, external medium, drug-lipid molar ratio and concentration of ammonium sulphate were evaluated for identification of factors having significant effect on values of dependent variables. The results of univariate analysis indicated that concentration of ammonium sulphate, drug loading pH and lipid-molar ratio had significant effect on aforementioned dependent responses. The liposomal formulations prepared with ammonium sulphate as transmembrane gradient (similar to that of clinically approved liposomal doxorubicin hydrochloride) showed characteristic DOX sulphate nanoprecipitation in electrodense soluble VCR sulphate present within coffee-bean shaped vesicles. The morphological characteristics of the formulations prepared with variations in the transmembrane gradient, lipid composition and temperature of drug loading exhibited different morphologies as compared to standard homogeneity. The in-vitro release studies exhibited staggered profile for DOX while having mixed profile for VCR at tested pH conditions with each drug presenting independent release profiles. The three causal variables having significant effect on the CQAs were then simultaneously varied and evaluated for their individual as well as interaction effect. The DOE studies showed that 350 mM ammonium sulphate, drug loading at pH 5.5 and lipid ratio of 56.55:38.19:5.26 (HSPC: Cholesterol: mPEG-2k-DSPE) were optimal for attainment of the desired product profiles. Further, variations in the CQAs were

traced and correlated with the physico-chemical properties as well as chemical structure of the two drugs. Thus, optimal development of dual drug loaded nanoliposomes should entail understanding the properties of therapeutic agents along with rationale-based evaluation of various causal independent factors for imparting the desired physicochemical properties. Such careful coupling of drug properties along with carrier properties would be essential in ascertaining the intended biological fate of the formulation and achieving the desired anti-neoplastic outcomes. Importantly, the present development strategy was further evaluated for in-vitro as well as in-vivo properties and results showed significantly improved therapeutic efficacy as compared to clinically approved liposomal doxorubicin hydrochloride. Additionally, the current research approach presented the rationale-based developmental plan of stable therapeutically effective combinatorial nanoliposomes having ease of scalability to cGMP scales.

7.5 References

1. Beltrán-Gracia E, López-Camacho A, Higuera-Ciapara I, Velázquez-Fernández JB, Vallejo-Cardona AA. Nanomedicine review: clinical developments in liposomal applications. Cancer Nanotechnology. 2019;10(1):11.

2. Pestana RC, Ibrahim NK. Cancer Treatment Modalities Systemic and Locoregional Approaches: Challenges and Opportunities of Multidisciplinary Approaches. Locoregional Radionuclide Cancer Therapy: Springer; 2021. p. 17-37.

3. Leary M, Heerboth S, Lapinska K, Sarkar S. Sensitization of drug resistant cancer cells: a matter of combination therapy. Cancers. 2018;10(12):483.

4. Silva CO, Pinho JO, Lopes JM, Almeida AJ, Gaspar MM, Reis C. Current trends in cancer nanotheranostics: metallic, polymeric, and lipid-based systems. Pharmaceutics. 2019;11(1):22.

5. Zucker D, Marcus D, Barenholz Y, Goldblum A. Liposome drugs' loading efficiency: a working model based on loading conditions and drug's physicochemical properties. Journal of controlled release : official journal of the Controlled Release Society. 2009;139(1):73-80.

6. Mokhtari RB, Homayouni TS, Baluch N, Morgatskaya E, Kumar S, Das B, et al. Combination therapy in combating cancer. Oncotarget. 2017;8(23):38022.

7. Bulbake U, Doppalapudi S, Kommineni N, Khan W. Liposomal formulations in clinical use: an updated review. Pharmaceutics. 2017;9(2):12.

8. Gubernator J. Active methods of drug loading into liposomes: recent strategies for stable drug entrapment and increased in vivo activity. Expert opinion on drug delivery. 2011;8(5):565-80.

9. Yamauchi M, Tsutsumi K, Abe M, Uosaki Y, Nakakura M, Aoki N. Release of drugs from liposomes varies with particle size. Biological and Pharmaceutical Bulletin. 2007;30(5):963-6.

10. Meikle T, Drummond C, Separovic F, Conn C. Membrane-mimetic inverse bicontinuous cubic phase systems for encapsulation of peptides and proteins. Advances in Biomembranes and Lipid Self-Assembly. 25: Elsevier; 2017. p. 63-94.

11. Farzaneh H, Nik ME, Mashreghi M, Saberi Z, Jaafari MR, Teymouri M. A study on the role of cholesterol and phosphatidylcholine in various features of liposomal doxorubicin: From liposomal preparation to therapy. International journal of pharmaceutics. 2018;551(1-2):300-8.

12. Ayala A, Muñoz MF, Argüelles S. Lipid peroxidation: production, metabolism, and signaling mechanisms of malondialdehyde and 4-hydroxy-2-nonenal. Oxidative medicine and cellular longevity. 2014;2014.

13. Maritim S, Boulas P, Lin Y. Comprehensive analysis of liposome formulation parameters and their influence on encapsulation, stability and drug release in glibenclamide liposomes. International Journal of Pharmaceutics. 2021;592:120051.

14. Mu Q, Yu J, McConnachie LA, Kraft JC, Gao Y, Gulati GK, et al. Translation of combination nanodrugs into nanomedicines: lessons learned and future outlook. Journal of drug targeting. 2018;26(5-6):435-47.

15. Maiti K, Bhowmick S, Jain P, Zope M, Doshi K, Rajamannar T. Comparison of Physicochemical Properties of Generic Doxorubicin HCl Liposome Injection with the Reference Listed Drug. Anti-cancer agents in medicinal chemistry. 2018;18(4):597-609.

16. Ghosh S, Lalani R, Maiti K, Banerjee S, Patel V, Bhowmick S, et al. Optimization and efficacy study of synergistic vincristine coloaded liposomal doxorubicin against breast and lung cancer. Nanomedicine (London, England). 2020;15(26):2585-607.

17. Ghosh S, Lalani R, Maiti K, Banerjee S, Bhatt H, Bobde YS, et al. Synergistic co-loading of vincristine improved chemotherapeutic potential of pegylated liposomal doxorubicin against triple negative breast cancer and non-small cell lung cancer. Nanomedicine: Nanotechnology, Biology and Medicine. 2021;31:102320.

18. Ghosh S, Mukherjee B, Chaudhuri S, Roy T, Mukherjee A, Sengupta S. Methotrexate aspasomes against rheumatoid arthritis: optimized hydrogel loaded liposomal formulation with in vivo evaluation in Wistar rats. AAPS PharmSciTech. 2018;19(3):1320-36.

19. Ghosh S, Mondal L, Chakraborty S, Mukherjee B. Early Stage HIV Management and Reduction of Stavudine-Induced Hepatotoxicity in Rats by Experimentally Developed Biodegradable Nanoparticles. AAPS PharmSciTech. 2017;18(3):697-709.

20. Patel V, Lalani R, Vhora I, Bardoliwala D, Patel A, Ghosh S, et al. Co-delivery of cisplatin and siRNA through hybrid nanocarrier platform for masking resistance to chemotherapy in lung cancer. Drug delivery and translational research. 2020:1-20.

21. Bhatt P, Lalani R, Vhora I, Patil S, Amrutiya J, Misra A, et al. Liposomes encapsulating native and cyclodextrin enclosed paclitaxel: Enhanced loading efficiency and its pharmacokinetic evaluation. International Journal of Pharmaceutics. 2018;536(1):95-107.

22. Jain A, Jain SK. In vitro release kinetics model fitting of liposomes: An insight. Chemistry and physics of lipids. 2016;201:28-40.

23. Barenholz YC. Doxil®—the first FDA-approved nano-drug: lessons learned. Journal of controlled release. 2012;160(2):117-34.

24. Alexis F, Pridgen E, Molnar LK, Farokhzad OC. Factors affecting the clearance and biodistribution of polymeric nanoparticles. Molecular pharmaceutics. 2008;5(4):505-15.

25. Steichen SD, Caldorera-Moore M, Peppas NA. A review of current nanoparticle and targeting moieties for the delivery of cancer therapeutics. European journal of pharmaceutical sciences. 2013;48(3):416-27.

26. Immordino ML, Dosio F, Cattel L. Stealth liposomes: review of the basic science, rationale, and clinical applications, existing and potential. International journal of nanomedicine. 2006;1(3):297.

27. Abumanhal-Masarweh H, da Silva D, Poley M, Zinger A, Goldman E, Krinsky N, et al. Tailoring the lipid composition of nanoparticles modulates their cellular uptake and affects the viability of triple negative breast cancer cells. Journal of controlled release. 2019;307:331-41.

28. Wang X, Song Y, Su Y, Tian Q, Li B, Quan J, et al. Are PEGylated liposomes better than conventional liposomes? A special case for vincristine. Drug delivery. 2016;23(4):1092-100.

29. Renne MF, de Kroon AI. The role of phospholipid molecular species in determining the physical properties of yeast membranes. FEBS letters. 2018;592(8):1330-45.

30. Samimi S, Maghsoudnia N, Eftekhari RB, Dorkoosh F. Lipid-based nanoparticles for drug delivery systems. Characterization and biology of nanomaterials for drug delivery. 2019:47-76.

31. Markovic M, Ben-Shabat S, Aponick A, Zimmermann EM, Dahan A. Lipids and lipid-processing pathways in drug delivery and therapeutics. International journal of molecular sciences. 2020;21(9):3248.

32. Dong X, Wang W, Qu H, Han D, Zheng J, Sun G. Targeted delivery of doxorubicin and vincristine to lymph cancer: evaluation of novel nanostructured lipid carriers in vitro and in vivo. Drug delivery. 2016;23(4):1374-8.

33. Zucker D, Barenholz Y. Optimization of vincristine–topotecan combination—Paving the way for improved chemotherapy regimens by nanoliposomes. Journal of Controlled Release. 2010;146(3):326-33.

34. Wei X, Shamrakov D, Nudelman S, Peretz-Damari S, Nativ-Roth E, Regev O, et al. Cardinal role of intraliposome doxorubicin-sulfate nanorod crystal in doxil properties and performance. ACS omega. 2018;3(3):2508-17.

35. Wehbe M, Anantha M, Backstrom I, Leung A, Chen K, Malhotra A, et al. Nanoscale reaction vessels designed for synthesis of copper-drug complexes suitable for preclinical development. PLoS One. 2016;11(4):e0153416.

36. Dicko A, Tardi P, Xie X, Mayer L. Role of copper gluconate/triethanolamine in irinotecan encapsulation inside the liposomes. International journal of pharmaceutics. 2007;337(1-2):219-28.

37. Dicko A, Kwak S, Frazier AA, Mayer LD, Liboiron BD. Biophysical characterization of a liposomal formulation of cytarabine and daunorubicin. International journal of pharmaceutics. 2010;391(1-2):248-59.

38. Fritze A, Hens F, Kimpfler A, Schubert R, Peschka-Süss R. Remote loading of doxorubicin into liposomes driven by a transmembrane phosphate gradient. Biochimica et Biophysica Acta (BBA)-Biomembranes. 2006;1758(10):1633-40.

39. Song Y, Huang Z, Song Y, Tian Q, Liu X, She Z, et al. The application of EDTA in drug delivery systems: doxorubicin liposomes loaded via NH4EDTA gradient. International journal of nanomedicine. 2014;9:3611.

40. Kheirolomoom A, Mahakian LM, Lai C-Y, Lindfors HA, Seo JW, Paoli EE, et al. Copper− doxorubicin as a nanoparticle cargo retains efficacy with minimal toxicity. Molecular pharmaceutics. 2010;7(6):1948-58.

41. Wei X, Cohen R, Barenholz Y. Insights into composition/structure/function relationships of Doxil® gained from "high-sensitivity" differential scanning calorimetry. European Journal of Pharmaceutics and Biopharmaceutics. 2016;104:260-70.

42. Briuglia M-L, Rotella C, McFarlane A, Lamprou DA. Influence of cholesterol on liposome stability and on in vitro drug release. Drug delivery and translational research. 2015;5(3):231-42.

43. Cui J, Li C, Wang C, Li Y, Zhang L, Zhang L, et al. Development of pegylated liposomal vincristine using novel sulfobutyl ether cyclodextrin gradient: is improved drug retention sufficient to surpass DSPE-PEG-induced drug leakage? Journal of pharmaceutical sciences. 2011;100(7):2835-48.

44. Epand RM. Do proteins facilitate the formation of cholesterol-rich domains? Biochimica et Biophysica Acta (BBA)-Biomembranes. 2004;1666(1-2):227-38.

45. Zucker D, Marcus D, Barenholz Y, Goldblum A. Liposome drugs' loading efficiency: a working model based on loading conditions and drug's physicochemical properties. Journal of controlled release. 2009;139(1):73-80.

46. Cern A, Golbraikh A, Sedykh A, Tropsha A, Barenholz Y, Goldblum A. Quantitative structure-property relationship modeling of remote liposome loading of drugs. Journal of controlled release. 2012;160(2):147-57.

47. Nordström R, Zhu L, Härmark J, Levi-Kalisman Y, Koren E, Barenholz Y, et al. Quantitative Cryo-TEM Reveals New Structural Details of Doxil-Like PEGylated Liposomal Doxorubicin Formulation. Pharmaceutics. 2021;13(1):123.

48. Karadag A, Özçelik B, Sramek M, Gibis M, Kohlus R, Weiss J. Presence of electrostatically adsorbed polysaccharides improves spray drying of liposomes. Journal of food science. 2013;78(2):E206-21.

49. Beltrán-Gracia E, López-Camacho A, Higuera-Ciapara I, Velázquez-Fernández JB, Vallejo-Cardona AA. Nanomedicine review: clinical developments in liposomal applications. Cancer Nanotechnology. 2019;10(1):1-40.

50. Johnston MJ, Edwards K, Karlsson G, Cullis PR. Influence of drug-to-lipid ratio on drug release properties and liposome integrity in liposomal doxorubicin formulations. Journal of liposome research. 2008;18(2):145-57.

51. Caputo F, Clogston J, Calzolai L, Rösslein M, Prina-Mello A. Measuring particle size distribution of nanoparticle enabled medicinal products, the joint view of EUNCL and NCI-NCL. A step by step approach combining orthogonal measurements with increasing complexity. Journal of Controlled Release. 2019;299:31-43.

52. Ghosh S, Lalani R, Patel V, Bardoliwala D, Maiti K, Banerjee S, et al. Combinatorial nanocarriers against drug resistance in hematological cancers: Opportunities and emerging strategies. Journal of controlled release : official journal of the Controlled Release Society. 2019;296:114-39.

53. Maeda H. Toward a full understanding of the EPR effect in primary and metastatic tumors as well as issues related to its heterogeneity. Adv Drug Deliv Rev. 2015;91:3-6.

54. Gratton SE, Ropp PA, Pohlhaus PD, Luft JC, Madden VJ, Napier ME, et al. The effect of particle design on cellular internalization pathways. Proceedings of the National Academy of Sciences. 2008;105(33):11613-8.

55. Danaei M, Dehghankhold M, Ataei S, Hasanzadeh Davarani F, Javanmard R, Dokhani A, et al. Impact of particle size and polydispersity index on the clinical applications of lipidic nanocarrier systems. Pharmaceutics. 2018;10(2):57.

56. Jain AK, Thareja S. In vitro and in vivo characterization of pharmaceutical nanocarriers used for drug delivery. Artificial cells, nanomedicine, and biotechnology. 2019;47(1):524-39.

57. Angelova MI, Bitbol A-F, Seigneuret M, Staneva G, Kodama A, Sakuma Y, et al. pH sensing by lipids in membranes: The fundamentals of pH-driven migration, polarization and deformations of lipid bilayer assemblies. Biochimica et Biophysica Acta (BBA)-Biomembranes. 2018;1860(10):2042-63.

58. Joseph E, Singhvi G. Multifunctional nanocrystals for cancer therapy: a potential nanocarrier. Nanomaterials for drug delivery and therapy. 2019:91-116.

59. Gaikwad VL, Choudhari PB, Bhatia NM, Bhatia MS. Characterization of pharmaceutical nanocarriers: in vitro and in vivo studies. Nanomaterials for drug delivery and therapy: Elsevier; 2019. p. 33-58.

60. Lunardi CN, Gomes AJ, Rocha FS, De Tommaso J, Patience GS. Experimental methods in chemical engineering: Zeta potential. The Canadian Journal of Chemical Engineering. 2021;99(3):627-39.

61. Tolcher AW, Mayer LD. Improving combination cancer therapy: the CombiPlex® development platform. Future Oncology. 2018;14(13):1317-32.

62. Burade V, Bhowmick S, Maiti K, Zalawadia R, Ruan H, Thennati R. Lipodox®(generic doxorubicin hydrochloride liposome injection): in vivo efficacy and bioequivalence versus Caelyx®(doxorubicin hydrochloride liposome injection) in human mammary carcinoma (MX-1) xenograft and syngeneic fibrosarcoma (WEHI 164) mouse models. BMC cancer. 2017;17(1):405.

63. Fugit KD, Xiang TX, Choi du H, Kangarlou S, Csuhai E, Bummer PM, et al. Mechanistic model and analysis of doxorubicin release from liposomal formulations. Journal of controlled release : official journal of the Controlled Release Society. 2015;217:82-91.

64. Noble CO, Guo Z, Hayes ME, Marks JD, Park JW, Benz CC, et al. Characterization of highly stable liposomal and immunoliposomal formulations of vincristine and vinblastine. Cancer chemotherapy and pharmacology. 2009;64(4):741-51.